Theory of VDE and associated Hiro, Evans and halo currents*

Leonid E. Zakharov (PPPL)

in collaboration with

Sergei Gerasimov, JET Contributors[1] *(CCFE, UK) and Xujing Li (ICM&SEC, China)*

[1]**See the Appendix of F. Romanelli et al., Proceedings of the 25th IAEA Fusion Energy Conference 2014, Saint Petersburg, Russia**

DIII-D Physics Seminar
January 19, 2015, General Atomic, San Diego NJ

*This work is partially supported by US DoE contract No. DE-AC02-09-CH11466, by the Chinese National Magnetic Confinement Fusion Science Program 2011GB105003, and has been carried out within the framework of the EUROfusion Consortium and has received funding from the Euratom research and training programme 2014-2018 under grant agreement No 633053 and from the RCUK Energy Programme [grant number EP/I501045].

PPPL PRINCETON PLASMA PHYSICS LABORATORY

Abstract

The talk presents the theory, simulations and physics of VDEs, consistent with JET measurements of toroidal asymmetries in the plasma current and toroidal magnetic field flux (diamagnetic signal). In 2007, the Tokamak MHD (TMHD) theory introduced the Hiro currents and gave the explanation of the wall currents in JET (still called the "halo" currents, despite their opposite direction to measurements). Now, the JET data on diamagnetic signals support the explanation of the currents to the tiles surface, discovered earlier on DIII-D in VDEs and measured on many tokamaks, by the theory introduced Evans currents, related to the current of electron and ions released from the plasma shrinking core. While having similarity with the conventional "halo"-currents, the Evans currents are source-limited and do not contribute to the forces on the wall.

The formulated understanding of VDE, which excludes the halo-currents as the players, opens new approaches for measurements, numerical simulations, and deeper theory development for prediction of the disruption effects in ITER.

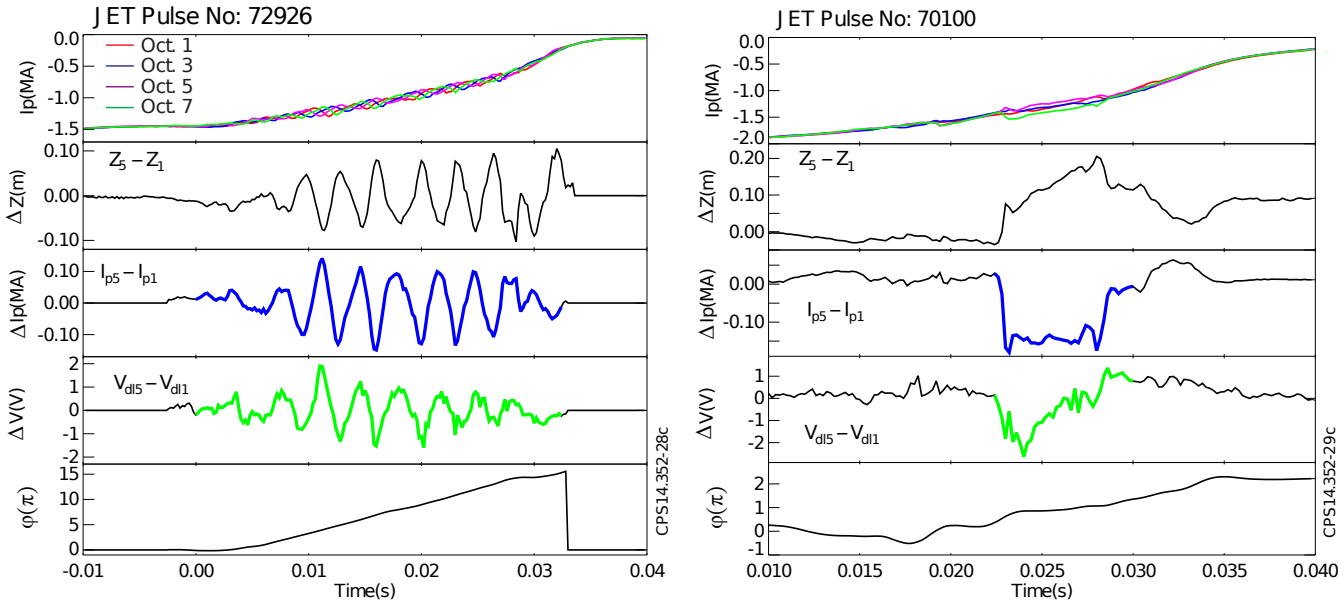

Contents

1 Attached poloidal currents on DIII-D (1991)

E.J. STRAIT, L.L. LAO, J.L. LUXON, E.E. REIS. "Observation of poloidal current flow to the vacuum vessel wall during vertical instabilities in the DIII-D tokamak", Nucl. Fusion v. 31 p. 527 (1991)

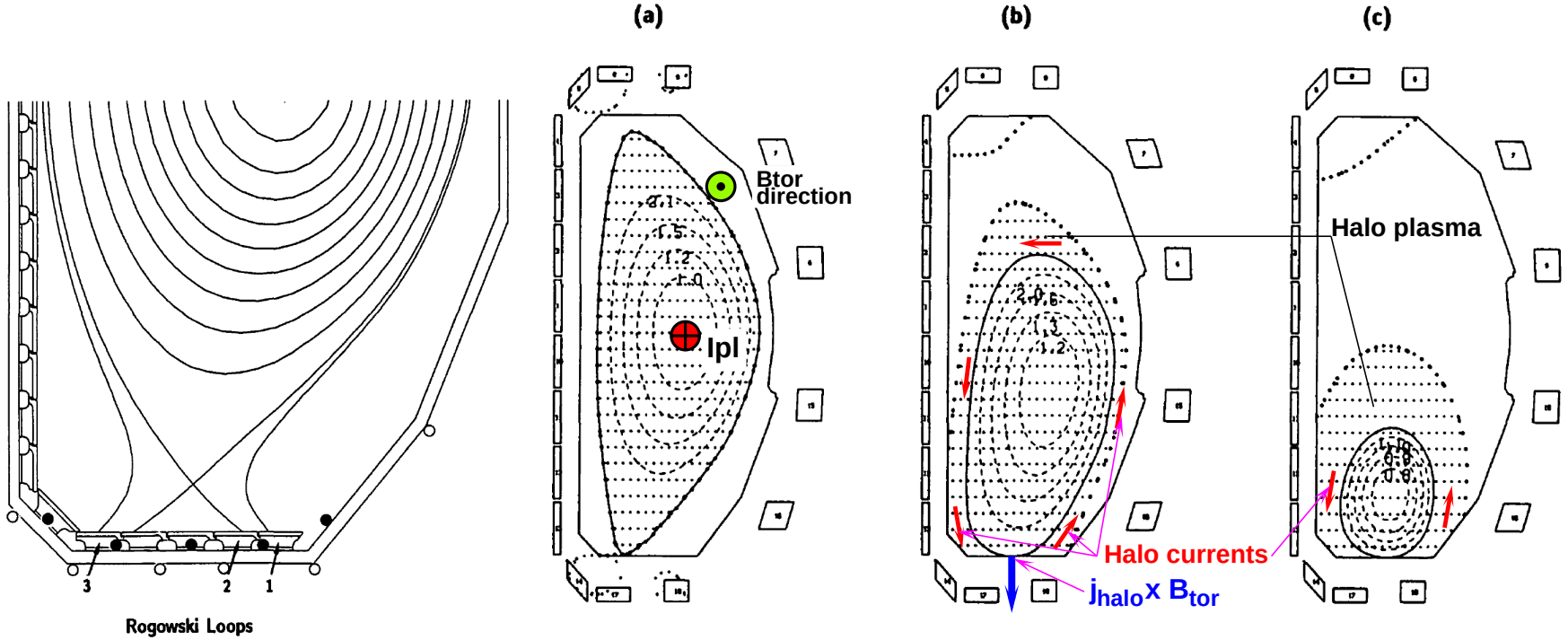

FIG. 3. Equilibrium flux plots from EFIT at three times during the vertical instability: (a) 2660 ms, (b) 2675 ms and (c) 2684 ms. Plasma current was allowed in the hatched region, including part of the SOL.

Large "halo" currents to tiles discovered far away from the last closed magnetic surface:

- ***Generated by EMF*** $-d(LI_{pl})/dt$ ***in the direction of plasma current due to plasma shrinking***
- ***Force-free in the halo zone***
- ***Flow along a short path in the wall across*** B_{tor} ***and exert a large vertical force to the wall***
- ***Balance the plasma vertically***

Driving voltage (EMF) for halo currents

From E.J. Strait et al, NF (1991):

6. DISCUSSION

The attached current measured by the armour tile Rogowski loops in the early stages of the vertical instability is probably driven by the vertical motion of the plasma. After the discharge comes into contact with the vacuum vessel wall during its downward motion, the cross-sectional area of the plasma begins to decrease (see Fig. 3). According to Lenz's law, the contraction of the plasma boundary across the toroidal magnetic field should induce a poloidal current which tends to conserve toroidal flux within the conducting plasma. The toroidal field points out of the page in Figs 1 and 3, so the sign of the observed current is consistent with this prediction. In the present example, the cross-sectional area decreases at a fairly constant rate of about 100-120 m^2/s in a toroidal field of 1.1 T, which, according to Faraday's law, would generate a poloidal electromagnetic force (EMF) of 110-130 V. The total toroidal flux contained in the discharge before the instability, about 2 Wb, can drive a much larger time integrated poloidal current (and hence a larger impulse to the vessel) than the diamagnetic flux of about 0.03 Wb.

The statement in red is incorrect:

$$U_{pol} \simeq -\frac{\partial \Phi}{\partial t} \simeq 0,$$

In blue is correct: there is only a toroidal (in fact along $\vec{B}$) EMF,

$$U_{tor} = U^{loop}_{voltage} \simeq -\frac{\partial \Psi^{edge}}{\partial t}$$

due to poloidal flux conservation.

It tries to preserve the plasma current when the plasma cross-section shrinks.

In VDE there is also an EMF due to plasma motion $\vec{V} \times \vec{B}^{Ext}$

2 Overview of theory.

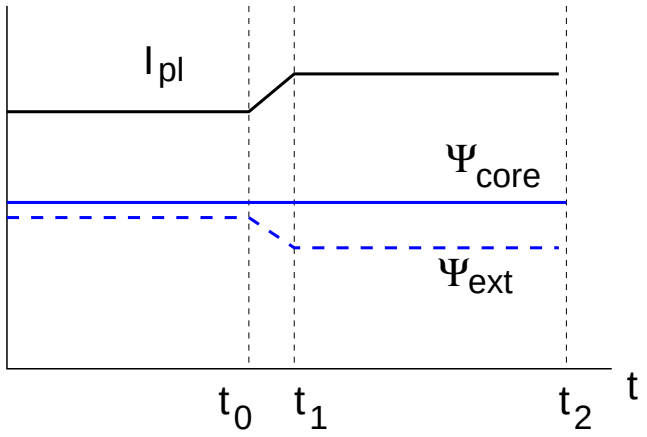

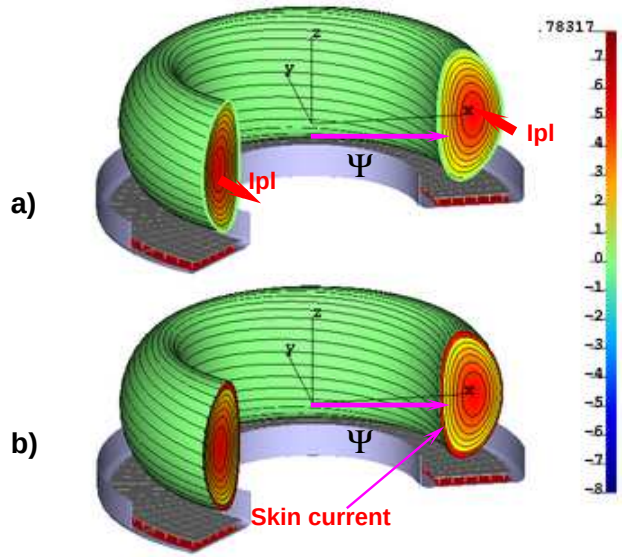

Simple example: sharp ramp up of I_{pl} by loop voltage $\dot{\Psi}_{ext}$

$$t_1 - t_0 \ll \quad \Delta t \equiv t_2 - t_1 \quad \ll \underbrace{\tau_{resistive}}_{\simeq 1\ s} \tag{2.1}$$

Skin layer

$$\Delta_m = 2\sqrt{\frac{t-t_1}{\mu_0 \sigma_\parallel}} \simeq \frac{2\sqrt{t-t_1}}{7T_{keV}^{3/4}}, \tag{2.2}$$

$$\Delta_m \simeq \frac{2\sqrt{\Delta t}}{7 \cdot 1_{keV}^{3/4}} \simeq 0.03 \cdot \sqrt{\frac{\Delta t}{0.01}} \ll a_0.$$

In fast evolution

1. $\Psi_{core} = \Psi(a_0 - \Delta)$ ***inside the core is preserved***
2. ***Diffusion of current density $j(a)$ does not affect the total currents***

$$I_{pl}(t_1 < t < t_2) \simeq I_{pl}(t_1)$$

3. ***I_{pl} is determined by flux conservation***

$$\Psi_{core}(t) = const$$

4. ***δ-functional model of current density δj is applicable***

$(\vec{V} \times \vec{B})$ as a driving EMF

It is right to neglect plasma inertia and consider only the equilibrium evolution

$$\tau_{MHD} \simeq \frac{R}{V_A} = \underbrace{\frac{R}{2.18 \cdot 10^6 B/\sqrt{n}}}_{<1\ \mu s} \ll \underbrace{\tau_{VDE}}_{\simeq 1\ ms} \ll \underbrace{\tau_{transport}}_{\simeq 0.1\ s} \ll \underbrace{\tau_{resistive}}_{\simeq 1\ s} \qquad (2.3)$$

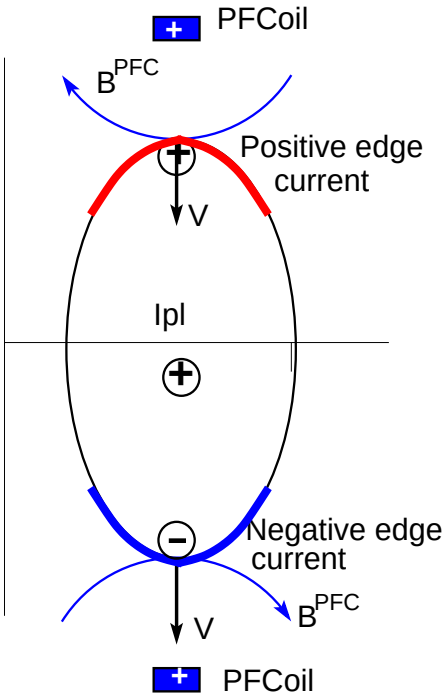

But

This is a SPECIAL, fast equilibrium evolution, which preserves the magnetic fluxes

Localized currents are automatically generated at the plasma surface (edge)

- ***negative*** ***(opposite to the plasma current) at the leading side***
- ***positive*** ***at the trailing side***

$$-\frac{\partial \vec{A}^{i,surf}}{\partial t} \underbrace{-\frac{\partial \vec{A}^{pl,core}}{\partial t} + V B_{pl} \vec{e}_\varphi}_{vanishes\ for\ m/n=1/0} + \underbrace{\vec{V} \times \vec{B}^{PFC}}_{Driving\ EMF} - \nabla \phi_E^{surf} = \frac{\vec{j}}{\sigma} \qquad (2.4)$$

The TMHD model used for this talk implements (2.3) into a rigorous set of equations

Surface currents in tokamaks

The generation of the surface (edge) currents is the fundamental tokamak MHD effect

Plasma electrons preserve the alignment of the plasma surface with the magnetic field

$$(\vec{B}\cdot\nabla\sigma_{\|})\simeq(\vec{B}\cdot\nabla T_e)\simeq 0, B_{normal}\simeq 0$$

- ***Without them the tokamak plasma would not exist - it would be always unstable***
- ***It is a fundamental effect of the real plasma - the plasma"resistivity" determines only the thickness of the current layer.***
- ***The perturbed plasma generates the same value of the edge current independent of plasma resistivity - works as a current generator***

The simple, δ-functional model of the surface (edge) currents is perfect to predict the most robust MHD effects in the tokamak plasma

The inductive effects are not related to the theoretical model of "ideal conductivity"

2.1 The δ-functional surface current model

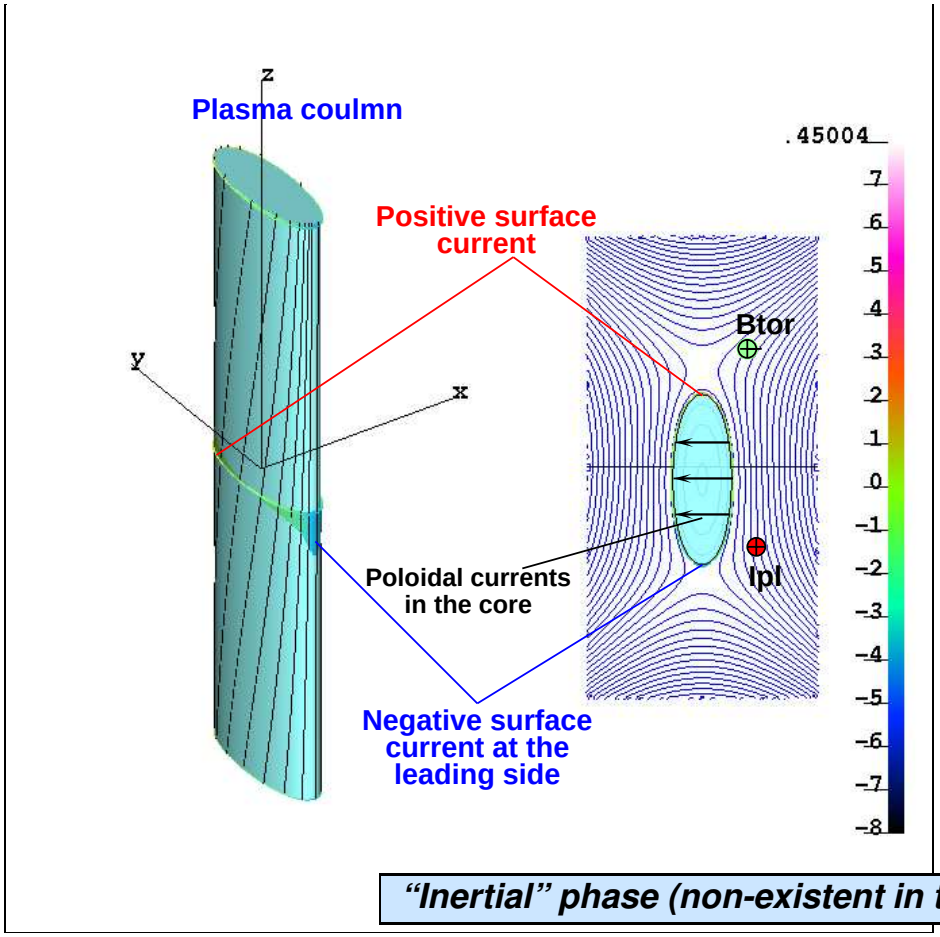

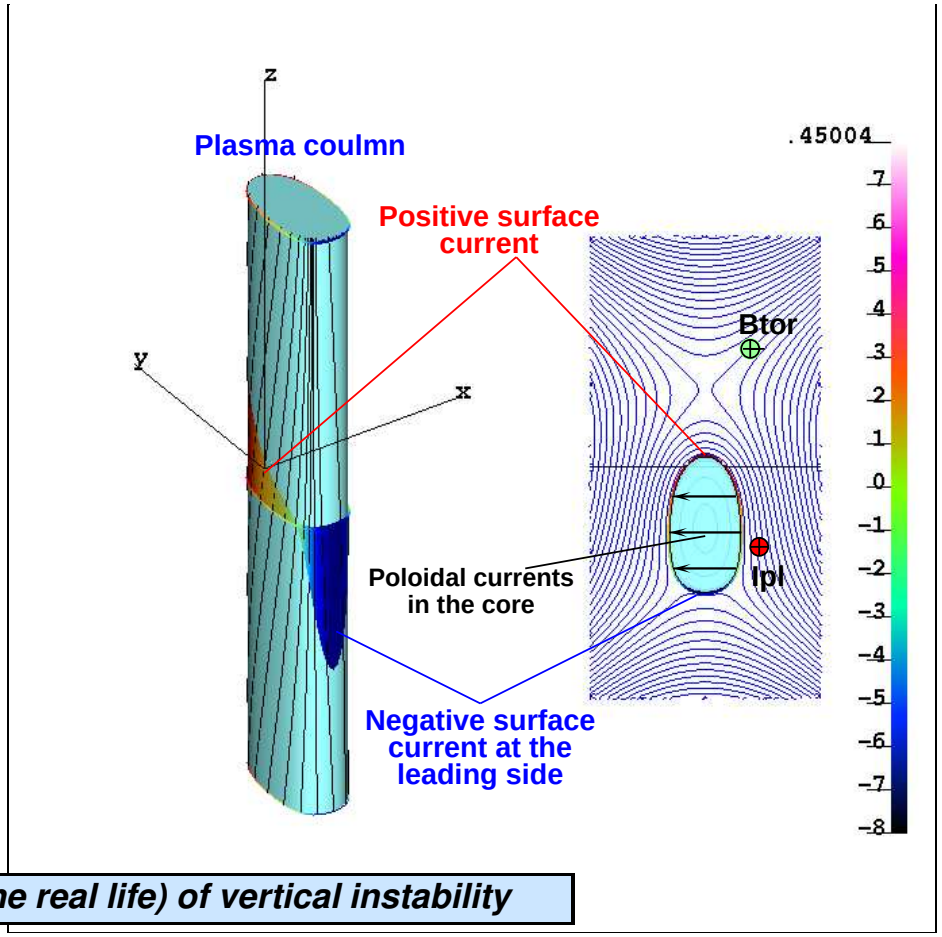

"Inertial" phase (non-existent in the real life) of vertical instability

1. ***Equilibrium in the core with flux conservation determines the distribution of surface currents.***
2. $\oint(\vec{\imath}\times\vec{B}_{pol})dS \;\propto\; \delta z_{pl} I_{pl}\vec{e}_z$ ***force is applied to the surface currents*** $\vec{\imath}$ ***in the direction of*** δz_{pl}
3. ***Weak poloidal currents*** $\vec{j}_{pol} = (\nabla\tilde{F}\times\vec{e}_z)$***, are generated in the core. They enter the plasma edge and make the surface currents force-free.***
4. ***The*** $(\vec{j}_{pol}\times\vec{B}_{tor})$ ***force in the core is compensated by plasma inertia. It advances the plasma shape.***

2.2 Toroidal Hiro currents along plasma facing surface

On the way to the wall, the plasma faces the tiles

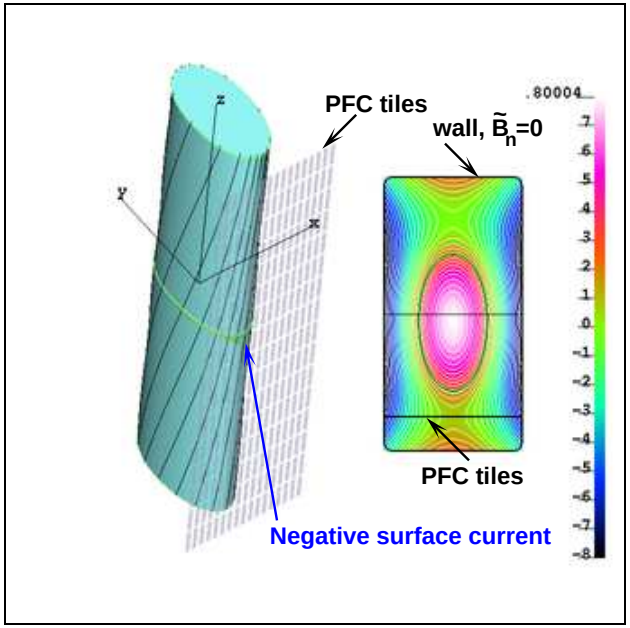

Initial plasma displacement

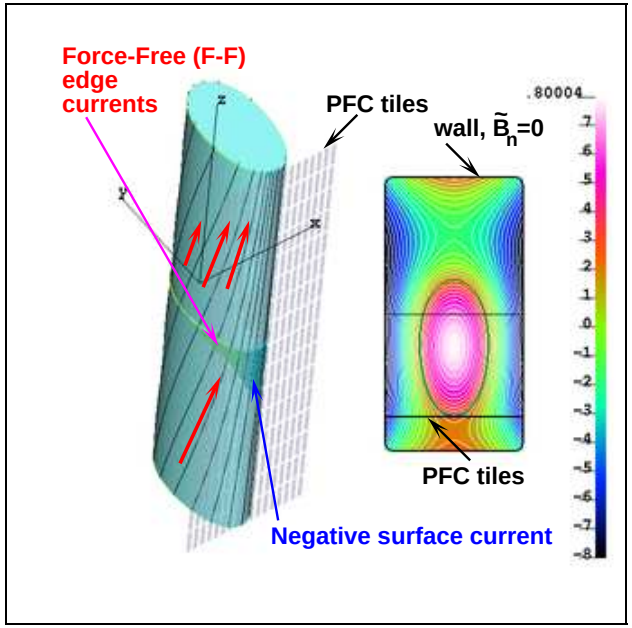

Negative surface current at the leading edge

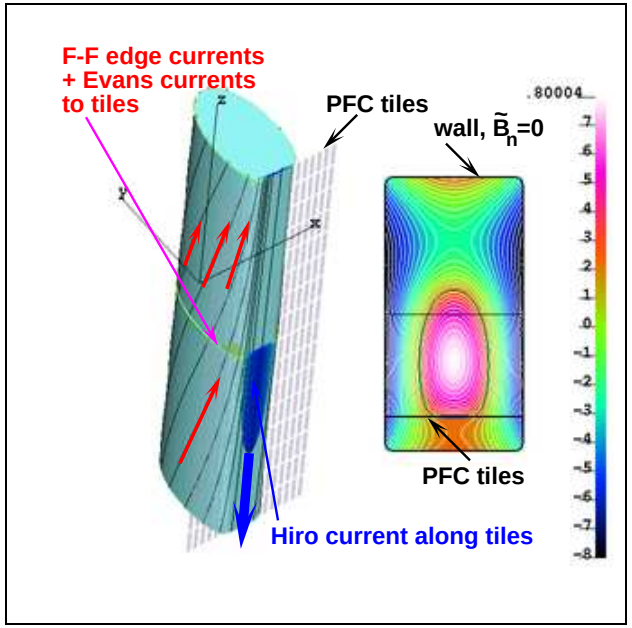

Hiro, Evans currents, formation of two Y-points

Predicted by the TMHD theory

(a) surface currents at the plasma boundary
(b) Hiro currents along the tile surface in the toroidal direction
(c) Evans currents from the plasma edge to the tile surface are well reproduced by the new VDE code.

Conventional compensation currents are driven during shrinkage of the plasma cross-section

Intermediate equilibrium maintained by the Hiro currents

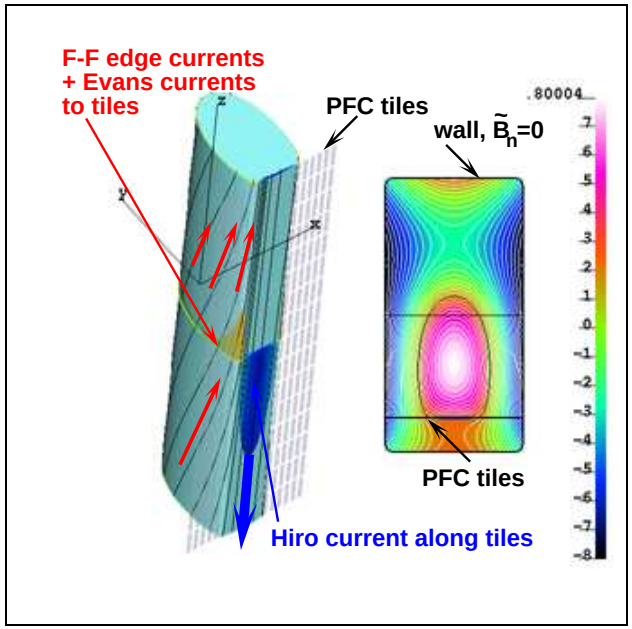

Hiro currents apply the force to tiles

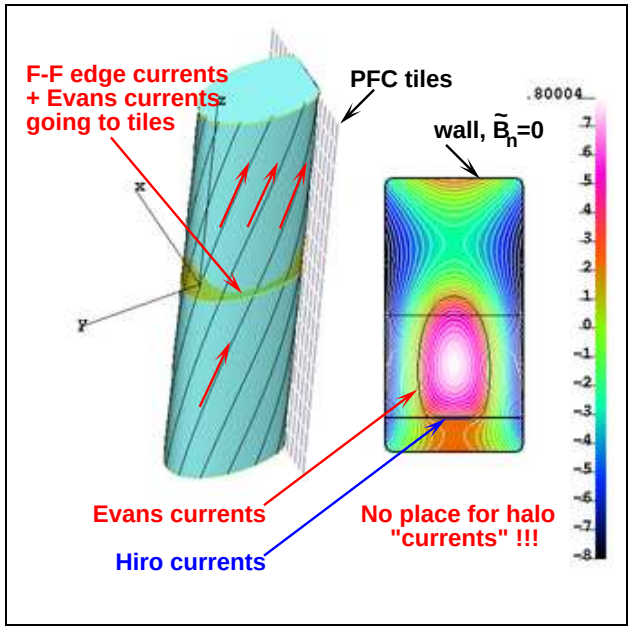

Evans currents. No place for the "halo" currents

Plasma shrinking due to decay of Hiro currents

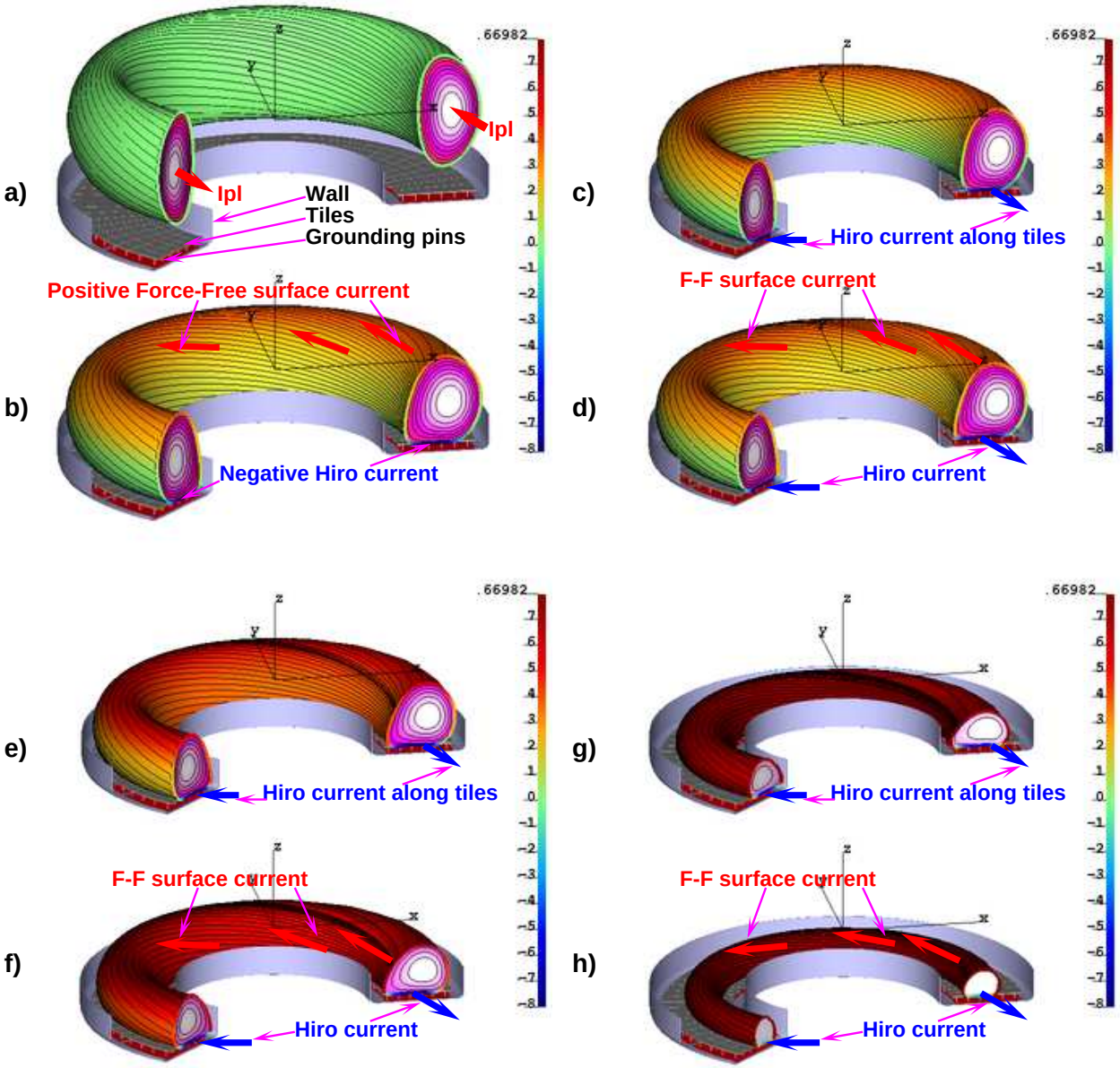

Hiro currents a automatically generated by $(\vec{V} \times \vec{B})$ ***to maintain the equilibrium***

During plasma shrinking I_{pl} ***decays***

The poloidally symmetric compensation current at the plasma edge

$$I^{FF} \simeq -I^{Hiro} + I^{V_{loop}}$$

At the later stage the contribution of $I^{V_{loop}}$ ***enhances the darkness of the color of the total edge current*** I^{FF}

On the way, the kink mode m/n=1/1 can be developed

2.3 Beyond the $\delta-$functional current model

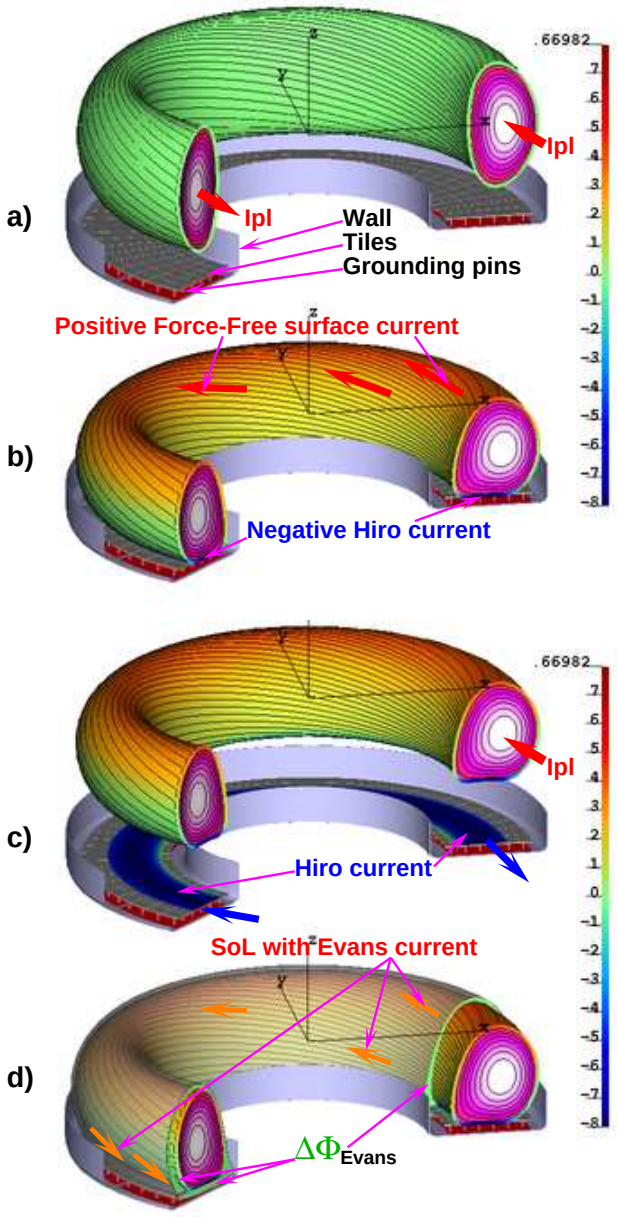

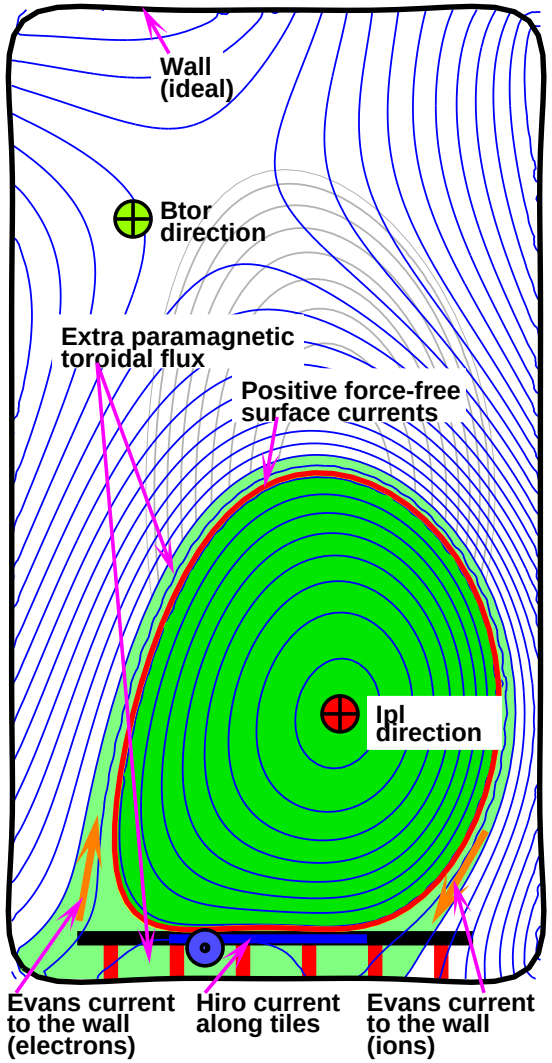

Resistive thickness of the F-F currents

$$\Delta^{FF} \simeq 2\sqrt{\frac{t}{\mu_0 \sigma_{\|}}} \simeq \frac{2\sqrt{t_s}}{7T_{keV}^{3/4}}$$

The shrinking plasma core releases the plasma particles and creates the halo zone

The Evans currents in the halo zone are a fraction of the I^{FF} current, and are limited by

$$I_{pol}^{Evans} < 2e\frac{dN_e}{dt}$$

The Evans currents to the tiles surface are driven by the loop voltage and observed as the currents to the tiles surface

There is no place for "halo" currents beyond the halo zone created from plasma core particles

Being similar to the halo currents, the Evans currents are the side effect of MHD instability

2.4 Xiong tiles on EAST

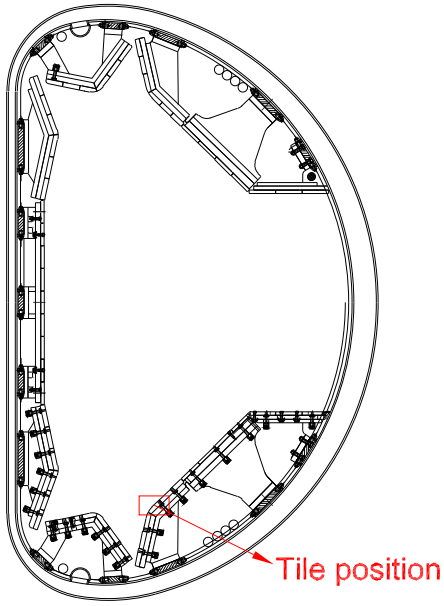

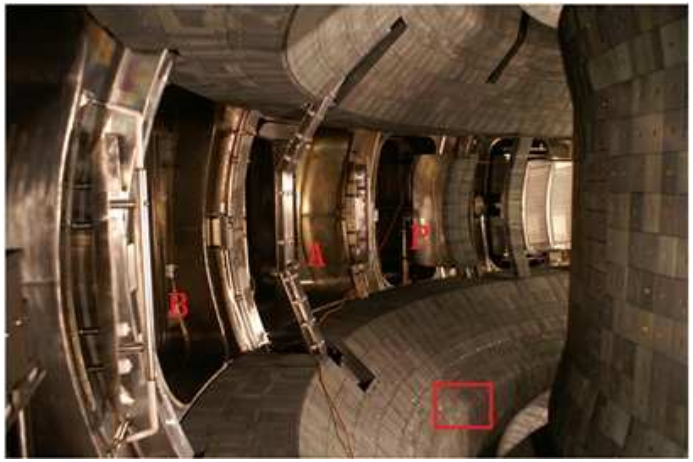

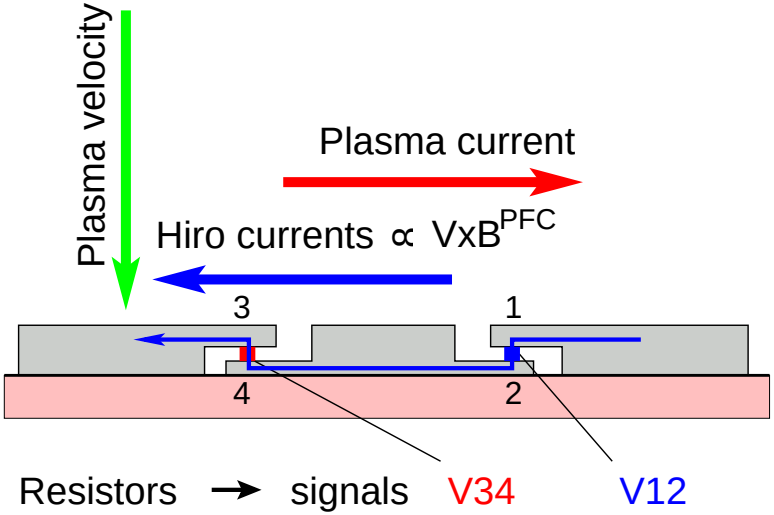

Two resistors between 3 shaped Mo tiles mounted through the thermal contact on a 2 cm thick copper heat sink plate, point-wise grounded

4 types of currents can be distinguished by the Xiong tiles.

First measurements of Hiro currents in VDE

Toroidal Hiro currents ($\simeq 0.8kA$), opposite to the plasma current, were measured on EAST in May 2012 for the first time in an axisymmetric VDE

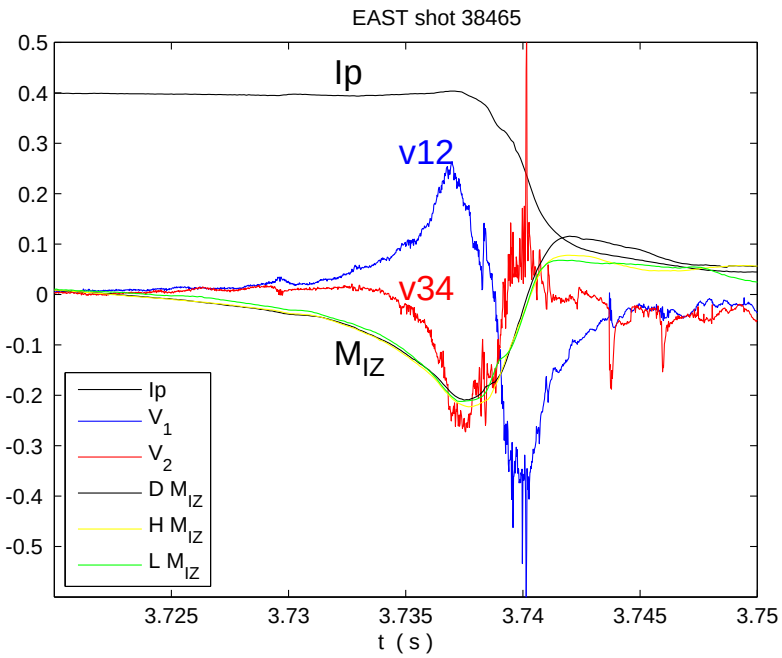

Downward VDE

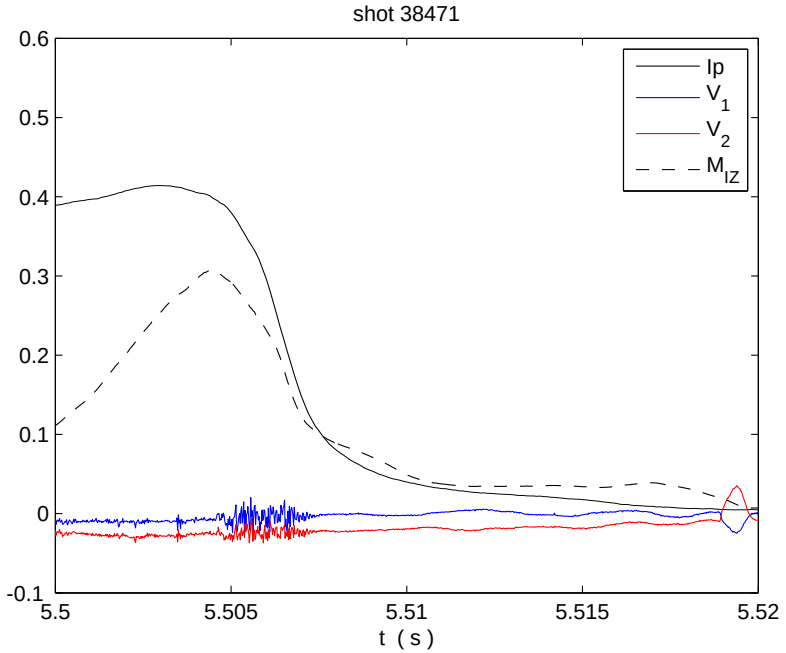

Upward VDE

No toroidal asymmetry, n=0, Ipl and Mirnov signals from three cross-sections are identical

Hiro currents in n=0 VDE are NOT SHARED between plasma and the tiles.

2.5 VDE as a current and voltage generator

1. ***VDE instability, acting as a current generator*, excites**
   (a) **the Hiro currents I^{Hiro} in the wetting zone of the plasma facing structures, and**
   (b) **the Force-Free edge currents $I^{FF} = -I^{Hiro} + I^{V_{loop}}$**
2. ***The Hiro currents provide the plasma equilibrium and exert the forces on the vessel.***
   (All other currents are not the players in forces on the vessel)
3. ***Plasma motion into the tiles is necessary* to maintain the necessary level of Hiro currents**
4. ***During the shrinkage of the plasma cross-section***
   (a) **The"halo"-zone is created from the ions and electrons released from the plasma core**
   (b) **The loop voltage outside the LCS drives the FF Evans currents in the halo zone along the open field lines**
   (c) **The Evans currents to the tile surface can be measured as the tile pins current**

The Evans current is the source limited ion and electron

$$I_{pol}^{Evans} < 2e\frac{dN_e}{dt}, \quad N_e \equiv \int n_e dV_{olume} \tag{2.5}$$

As the reference numbers

$$\begin{aligned} &\textbf{DIII-D}: \quad \int I^{Evans}(t)dt < 2eN_e \simeq 2\cdot 1.6\cdot 10^{-19}\cdot 3\cdot 10^{19}\cdot 20_{m^3} \simeq 200\ \textbf{[A}\cdot\textbf{s]}, \\ &\textbf{JET}: \quad \int I^{Evans}(t)dt < 2eN_e \simeq 2\cdot 1.6\cdot 10^{-19}\cdot 3\cdot 10^{19}\cdot 60_{m^3} \simeq 600\ \textbf{[A}\cdot\textbf{s]} \end{aligned} \tag{2.6}$$

3 JET VDEs. Wall Touching Kink Mode 1/1

Introduced in 2007 as a key element of disruptions

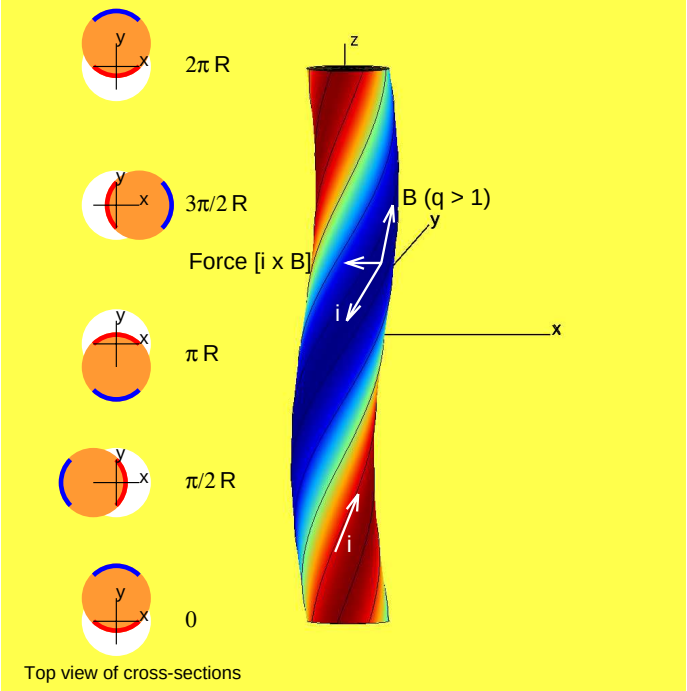

Hiro currents*

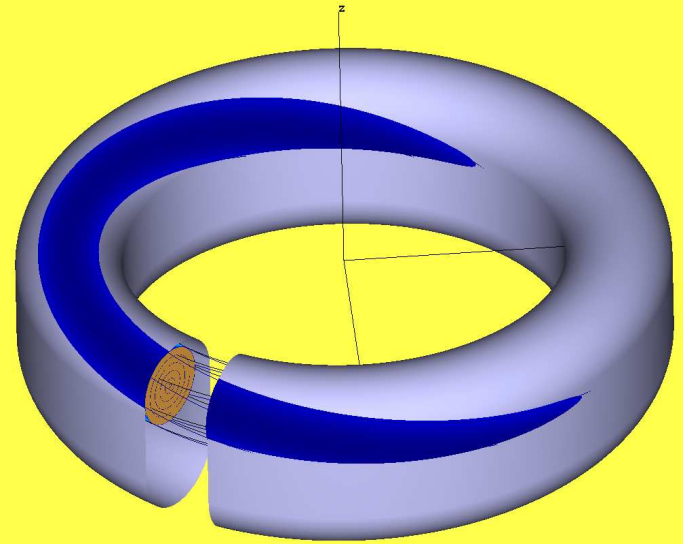

**named in the honor of Hironori Takahashi*

Only negative part of $i(\omega, \varphi)$ can be shared between plasma and the wall.

The m/n=1/1 WTKM in VDE always leads to asymmetry in plasma current measurements.

Hiro currents are predicted by theory of perturbed equilibrium

This makes the Hiro currents prediction unshakable.

Magnetic Diagnostic (1)

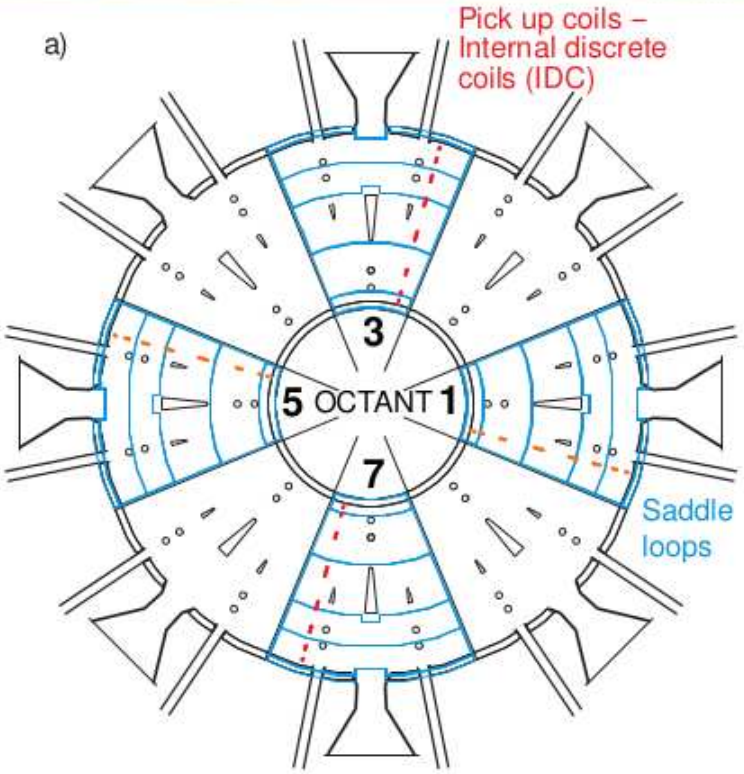

Plan view of JET vessel, showing the toroidal locations of **pick up coils** and **saddle loops**

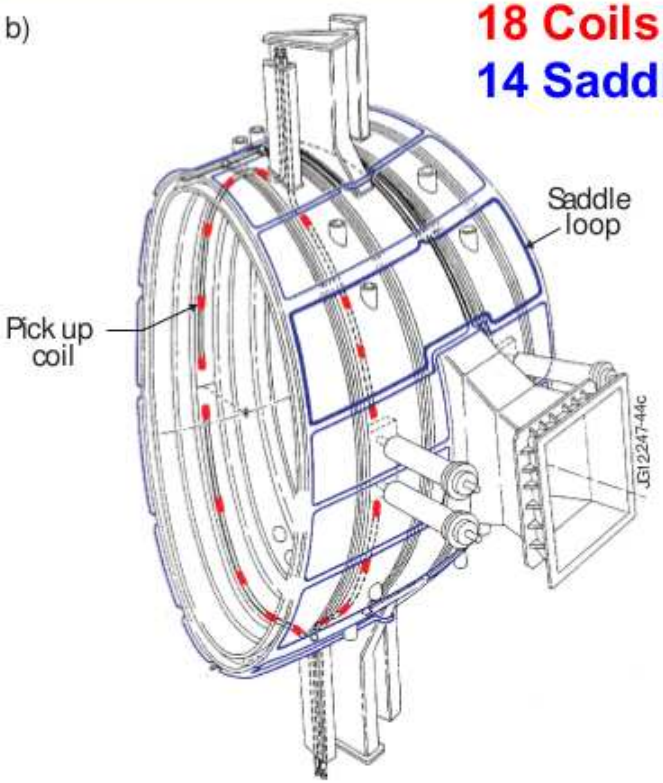

Each vessel octant was equipped with **pick up coils (IDC)** and **saddle loops**

The integrated signals are recorded regularly with 16-bit ADC at 5 kHz from 3/11/2005 onwards. *(The plasma current quench durations > 10ms)*

Magnetic Diagnostic → Current Moments

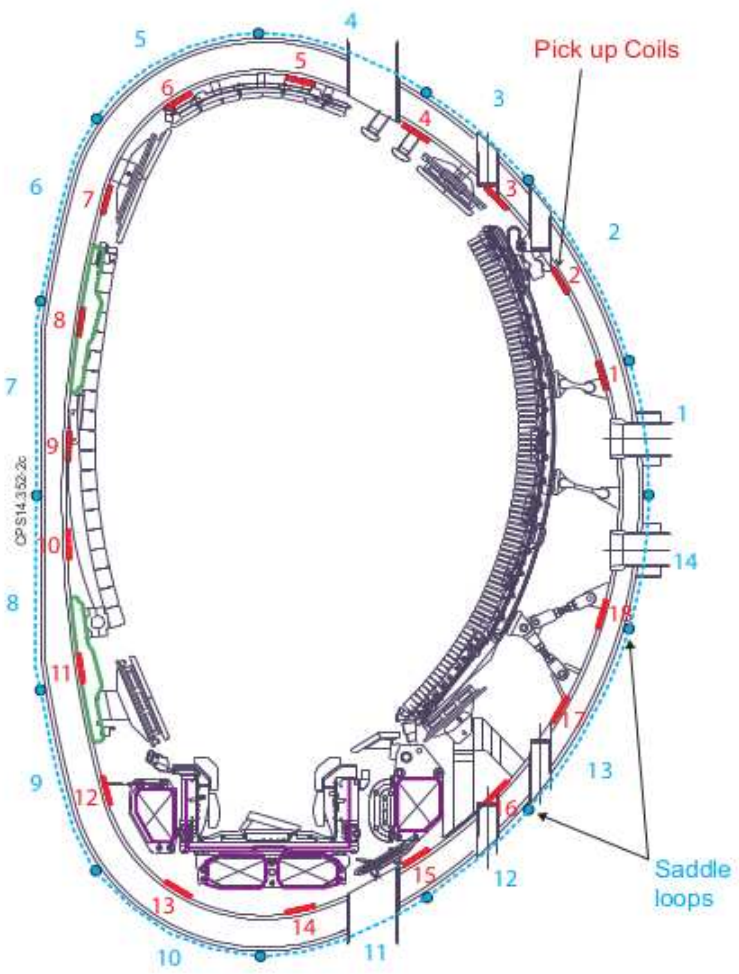

Plasma Current Calculation ⇨

$$\mu_0 I = \oint \vec{B}\vec{dl}$$

⇩

$$I_p = \frac{1}{\mu_0}\sum_{i=1}^{18} B_{\vartheta i} d_i - \sum_{i=1}^{4} n_{Di} I_{Di} - (I_{RRU} + I_{RRL})$$

First Plasma Current Moment Calculations ⇨

$$M_{IR} \equiv \int (R-R_o) J_\phi dR dZ$$

$$M_{IZ} \equiv \int Z J_\phi dR dZ$$

⇩

$$M_{IZ} = \frac{1}{\mu_0}\left(\sum_{i=1}^{18} B_{\vartheta i} z_i d_i + \frac{1}{2\pi}\sum_{i=1}^{14} \Psi_i \ln\left(\frac{R_o}{r_i}\right)\right)$$

$$-\sum_{i=1}^{4} z_{Di} n_{Di} I_{Di} - (z_{RRU} I_{RRU} + z_{RRL} I_{RRL})$$

Divertor support structure and divertor PF coil cases are not included in calculations (~5% of Ip at disruption), because there are no reliable measurements. It does not affect the asymmetry calculation.

Magnetic Diagnostic – Diamagnetic Poloidal Loops

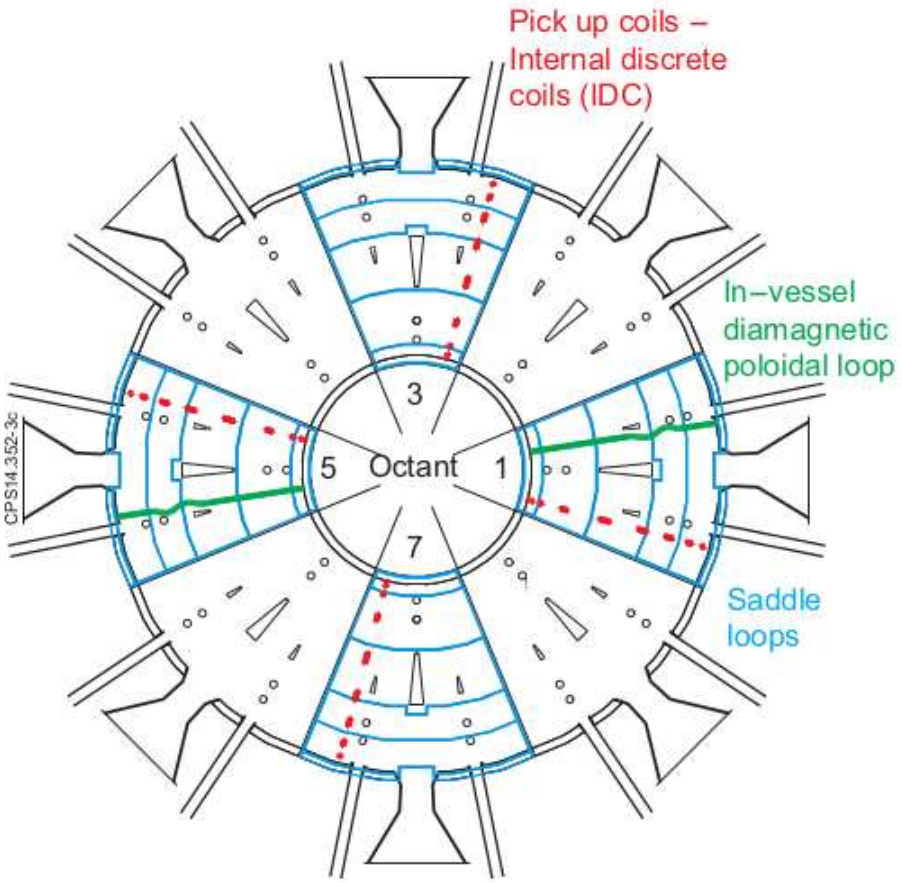

Plan view of JET vessel, showing the toroidal locations of **in-vessel diamagnetic poloidal loops**

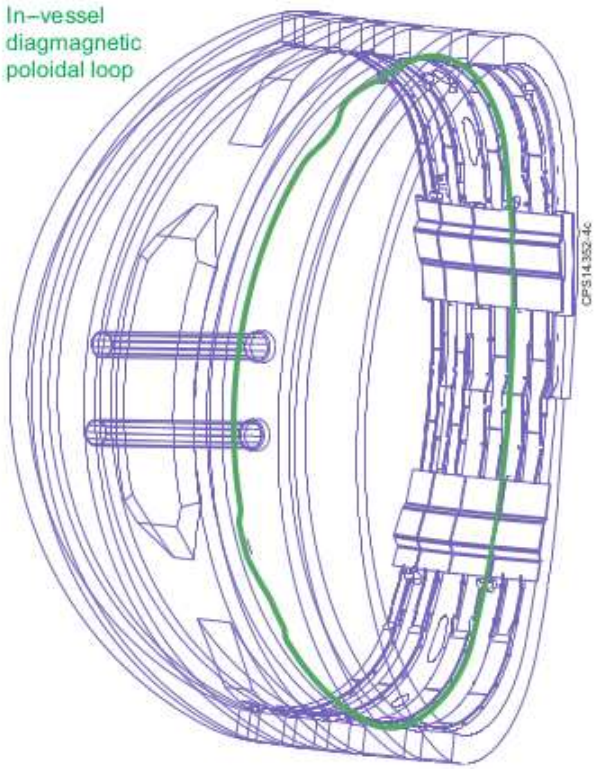

#1 and #5 octants equipped with **in-vessel diamagnetic poloidal loops**

Radial Vessel Displacement Diagnostic

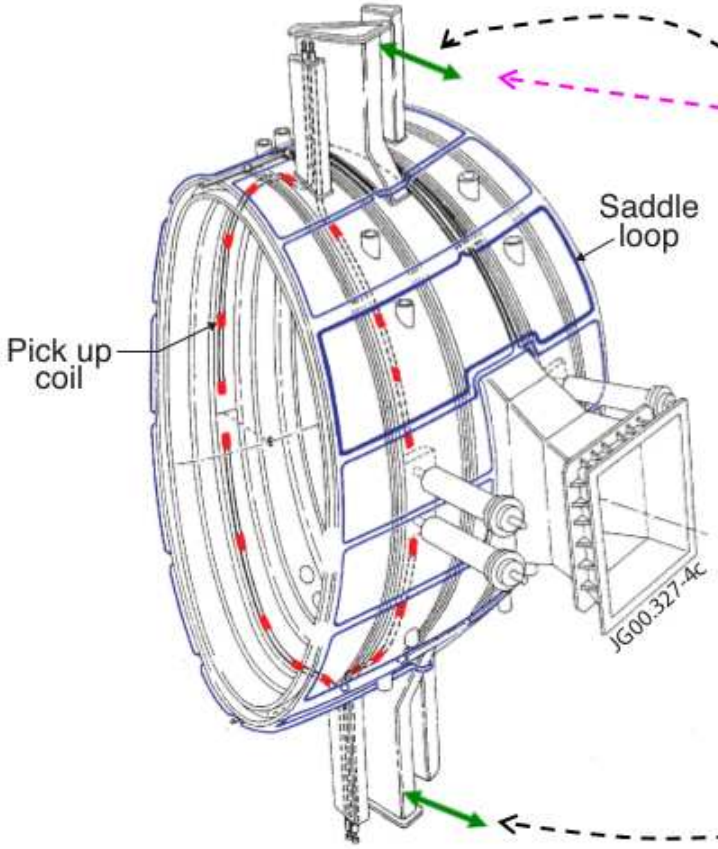

Displacement transducers

Displacement transducer

Transducers measure radial movement at vertical port of the each vessel octant with respect to mechanical structure

Vessel current during VDE, #38070

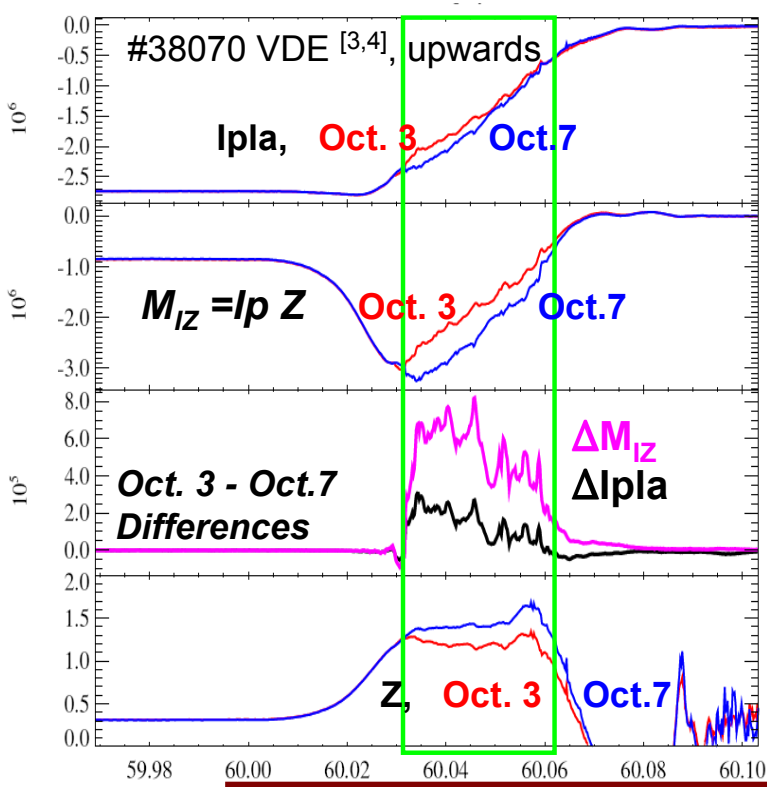

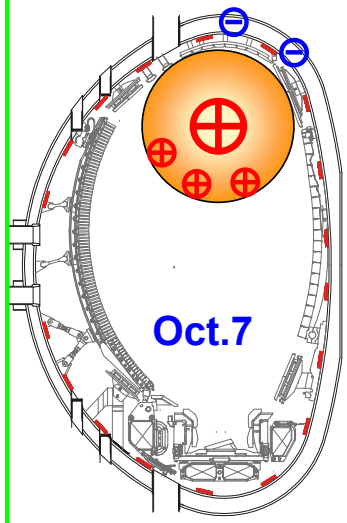

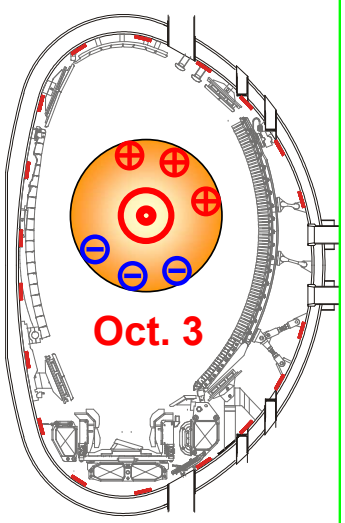

- In octant 7 the plasma is closer to top of the vessel than in octant 3.
- **The current from plasma flows on vessel in octant 7.**

The measured Ipla in octant 7 is higher then in octant 3 ➔ the missing vessel current in octant 7 is OPPOSITE to Ipla!

The "halo" current based interpretation predicts the opposite sign of asymmetry in the current measurement and contradicts JET Ipla's.

WTKM explained the toroidal asymmetry in Ipl on JET

Hiro current theory has amazing consistency with experiment in the sign of the effect and its time dependence. No tricks are necessary.

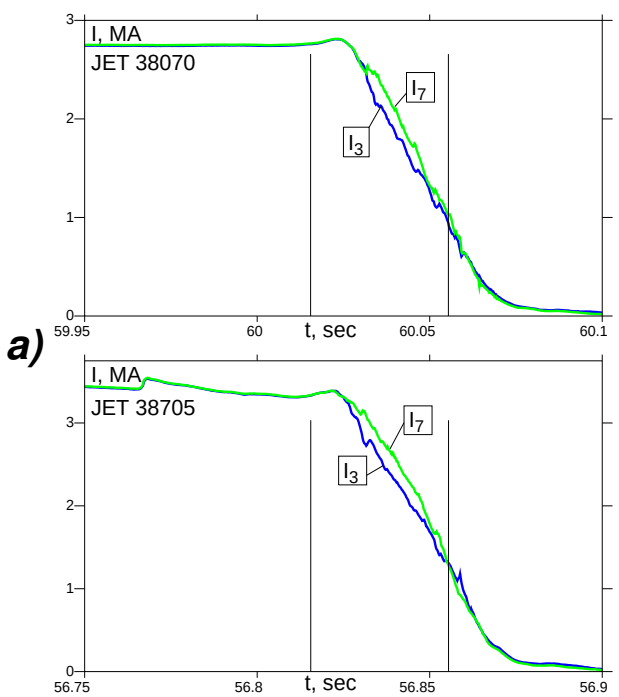

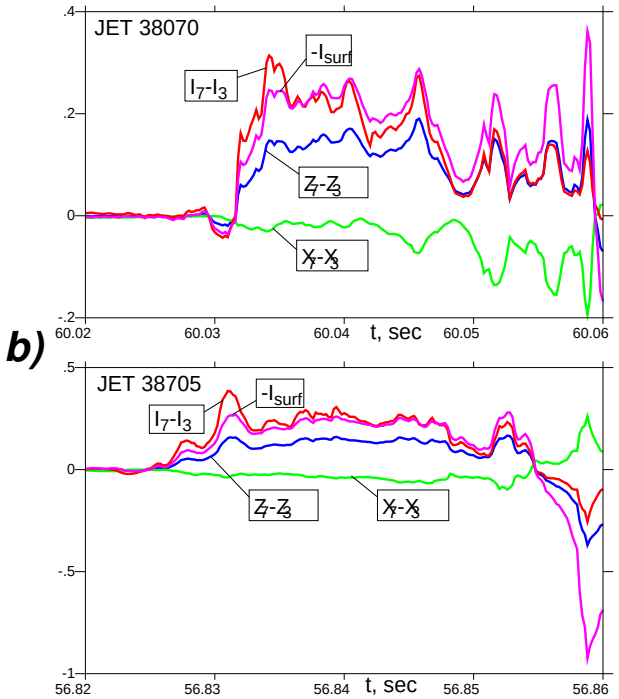

(a) Plasma currents $I_{3,7}$ in octants 3,7 on JET during the disruptions.
(b) $Z_7 - Z_3$ and $R_7 - R_3$, $I_7 - I_3$ and its prediction $-I^{surf}$ from the present theory.

$$I_{est}^{surf} \simeq -a\frac{4B_\varphi}{R_0\mu_0}\frac{\delta Z_{7,3}}{2} \ll I^{surf}, \quad Z_{7,3} \equiv \frac{1}{\mu_0 I_{pl}}\oint f B\tau dl \simeq \frac{1}{2}z_{p,7,3},$$
$$\mu_0\vec{\imath}_{11} = -2\xi_{11}\frac{B_\varphi}{R}\left(\mathbf{e}_\varphi + \frac{a}{R}\mathbf{e}_\theta\right), \quad I_{Hiro} \simeq I_{surf} = -4a\xi_{11}\frac{B_\varphi}{R\mu_0}. \qquad (3.1)$$

Hiro currents explain toroidal asymmetry in Ipl

100 % success in explanation of the sign of toroidal asymmetry on wall currents on JET

(in contrast to 100 % failure of "halo current"interpretations)

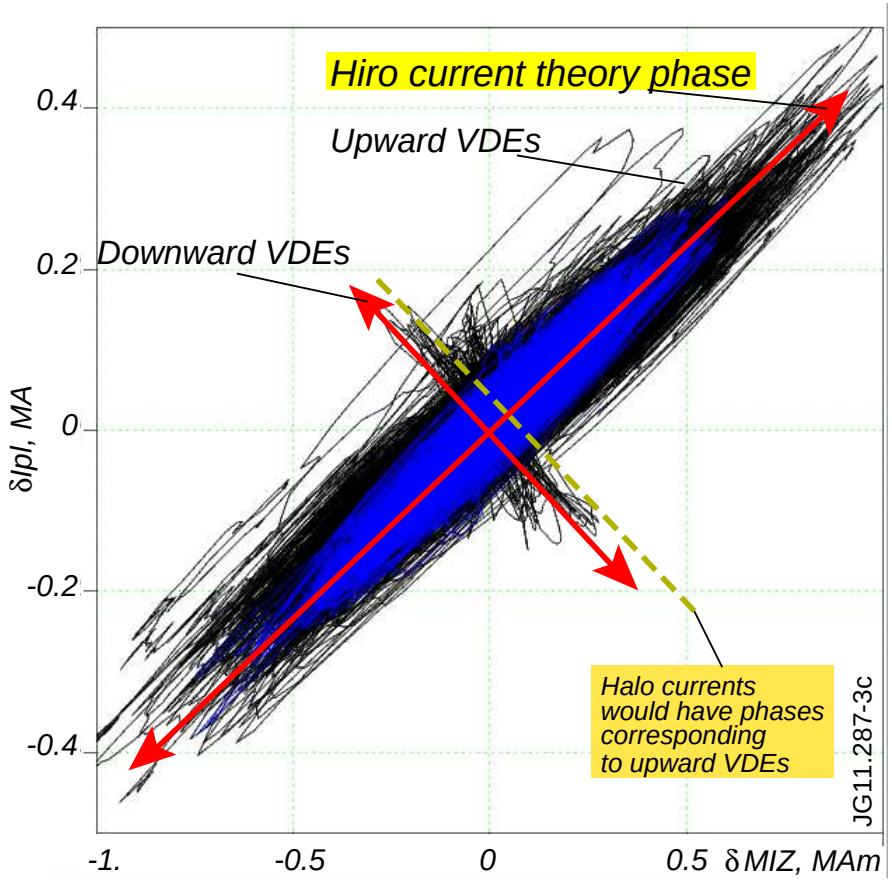

dB (Aug. 2014) for the Phase diagram

PSC	Octants	All cases	VDE
C-wall	3-7	4429	1673
C-wall	1-5	963	299
IL-wall	3-7	371	162
IL-wall	1-5	391	160

Vertical axis

$$\delta I_{pl} \equiv I_{pl}(\varphi+\pi,t) - I_{pl}(\varphi,t)$$

Horizontal axis:

$$\delta M_{IZ} \equiv M_{IZ}(\varphi+\pi,t) - M_{IZ}(\varphi,t)$$

Black color: $\varphi = 90^o$ **for Octants 7-3**
Blue color: $\varphi = 0^o$ **for Octants 1-5**

The currents in the wall measured on JET are the Hiro currents

3.2 JET asymmetry in the Diamagnetic signal

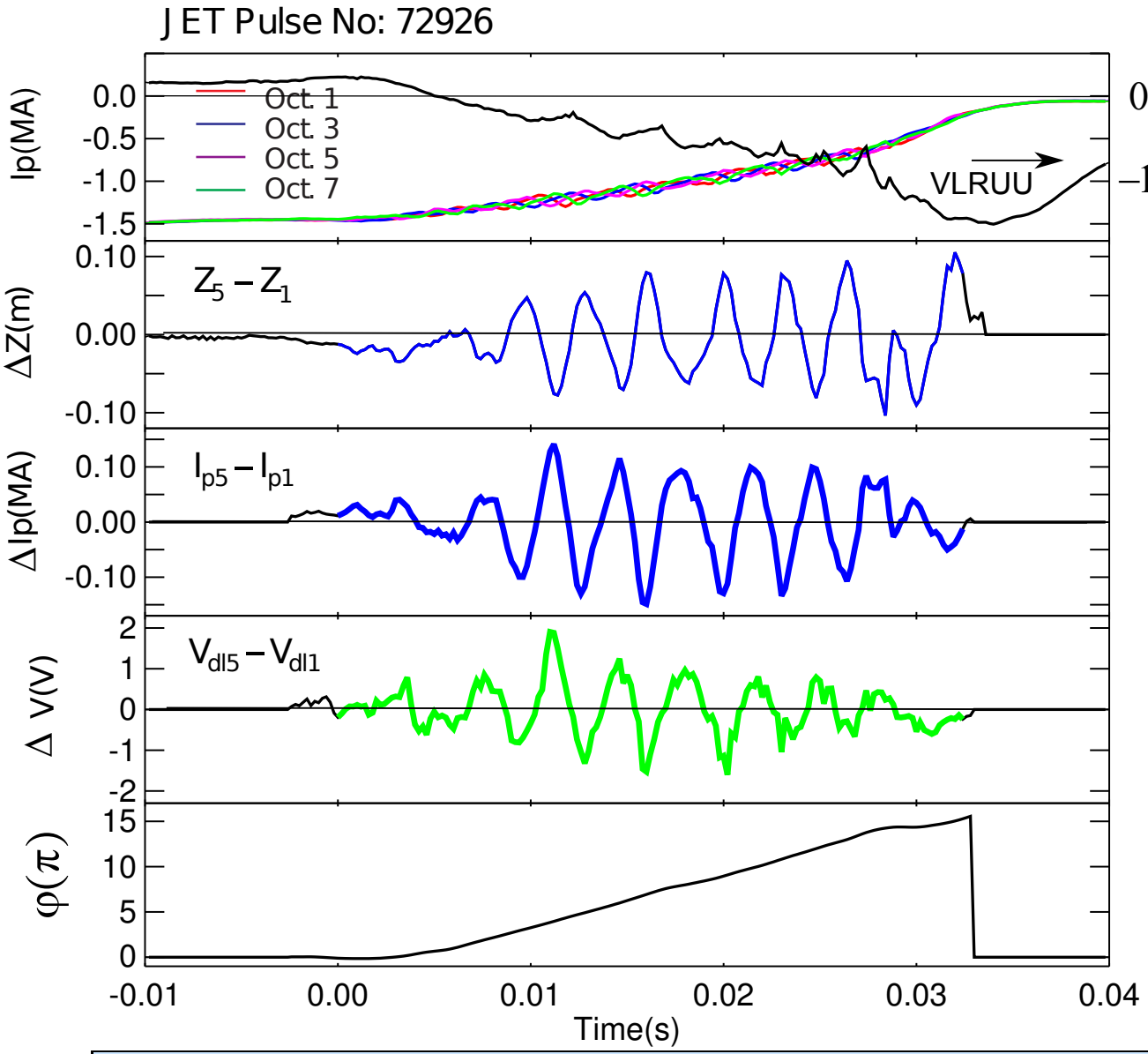

Rotating m/n=1/1 WTKM

Loop Voltage

$$U \simeq -50\ V$$

Kink 1/1 amplitude

$$\xi \simeq 5\ cm$$

Hiro currents

$$I^{Hiro} \simeq 0.2\ MA$$

Paramagnetic Voltage

$$|V_{pol}| = \left| -\frac{d\Phi_{tor}}{dt} \right| \simeq 1\ V$$

Period of rotation

$$\Delta t \simeq 3\ ms$$

Paramagnetic signal is consistent with expected locationof the halo zone near the wetting spot and the sign of Evans currents !!!

"Locked" m/n=1/1 WTKM on JET (Gerasimov 2014)

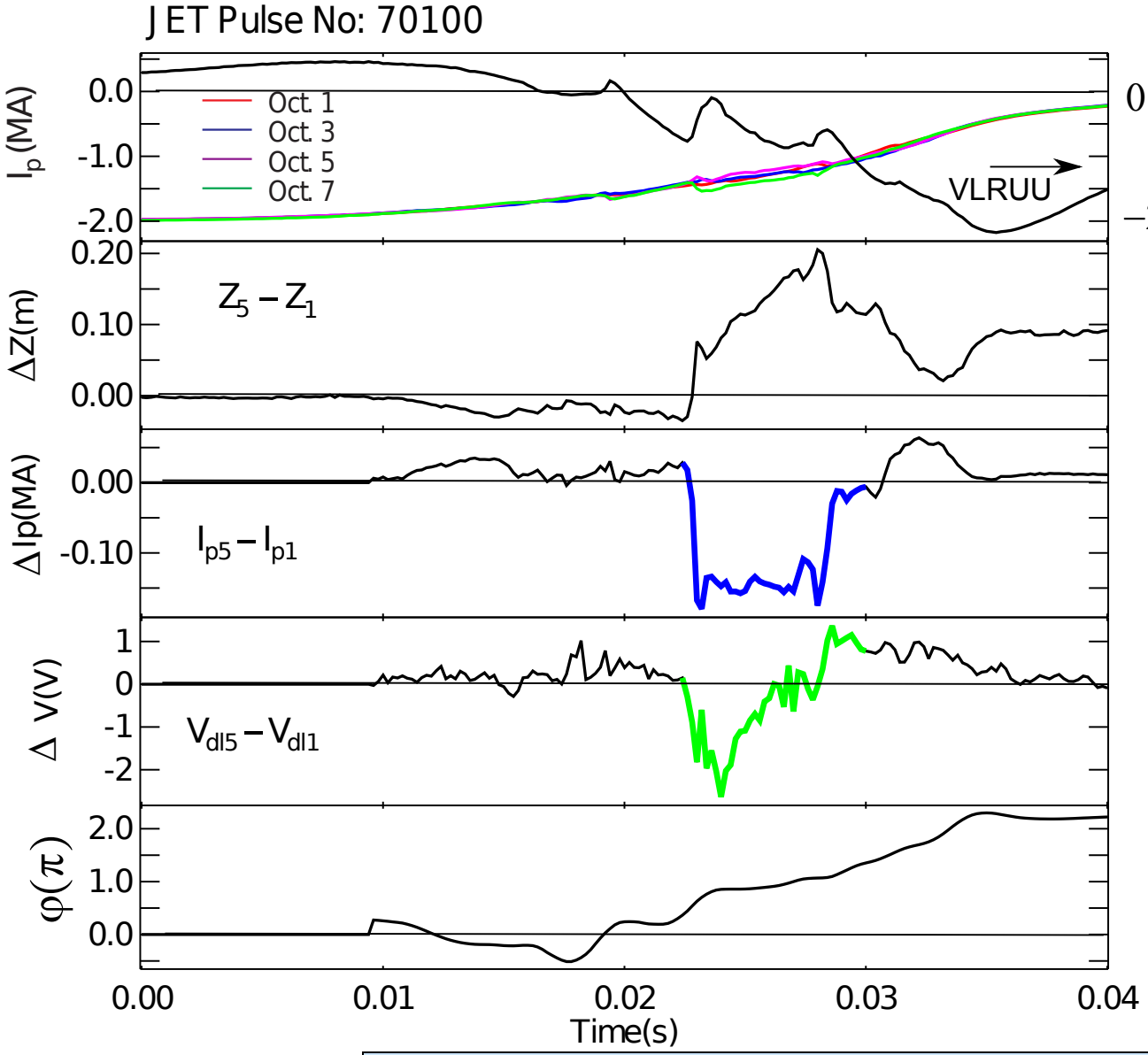

Loop Voltage

$$U \simeq -70\ V$$

Kink 1/1 amplitude

$$\xi \simeq 8\ cm$$

Hiro currents

$$I^{Hiro} \simeq 0.15\ MA$$

Period of rotation

$$\Delta t \simeq 25\ ms$$

Paramagnetic Voltage

$$|V_{pol}| = \left| -\frac{d\Phi_{tor}}{dt} \right| < 2\ V$$

The drop in time of Paramagnetic Signal may indicate the saturation the Evans currents !!!

The theory interpretation of $\delta\dot{\Phi}$ asymmetry

1. *The halo-zone is toroidally localized in the vicinity of the wetting zone*
2. *Both Hiro and Evans currents enter the wall structure (Hiro currents escape magnetic probes)*
3. *The Hiro currents are situated right after the plasma core edge which have the same Φ in all cross-sections*
4. *The Evans currents have a larger footprint and generate an extra paramagnetic flux*

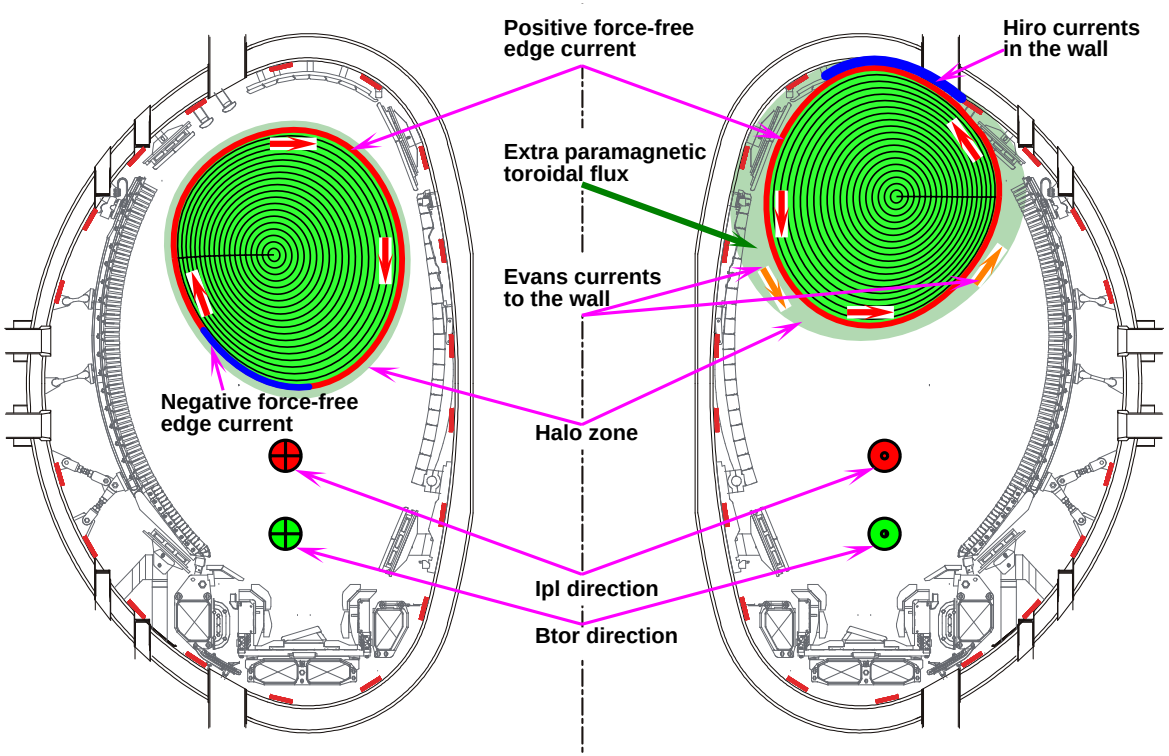

Theory suggests that Evans currents in the wetting zone are responsible for asymmetry in $\delta\Phi$

The relevant reference illustrative numbers

$< n_e >$	$3 \cdot 10^{19}$	- average core plasma density
V_{olume}	60 m^3	- plasma volume
t^{CQ}	$\simeq 25$ ms	- current quench time for assessment of $\dot{N}_e$
$Q = 2en_eV_{olume}$	600 A·s	- total particle charge

The source limitation on the Evans current

$$I^{Evans} \leq I^{S-Limit} \equiv 2e\frac{dN}{dt} = \frac{600}{0.025} \simeq 0.024\ MA. \tag{3.2}$$

For explanation of the $\delta\Phi$ asymmetry it is necessary to have

$$\mu_0 \frac{I^{Evans}}{L^{wet}} = \delta B_{tor} = \frac{\delta\Phi}{\delta S^{Evans}}. \tag{3.3}$$

For rotating mode 72926 $I^{S-Limit}$ is sufficient (the extra factor 2 is necessary)

$$\begin{aligned} I^{Evans}_{MA} &\simeq 2\frac{V_{pol}\Delta t}{2\pi\mu_0\delta S^{Evans}}L^{wet} \\ &\simeq 0.02 \cdot \frac{0.2}{\delta S^{Evans}_{m^2}} \cdot \frac{L^{wet}_m}{5} \end{aligned} \tag{3.4}$$

For the locked mode 70100 the limit is restrictive

$$I^{Evans}_{MA} \simeq \frac{\int V_{pol}dt}{\mu_0\delta S^{Evans}}L^{wet} \qquad \simeq 0.04 \cdot \frac{0.2}{\delta S^{Evans}_{m^2}} \cdot \frac{L^{wet}_m}{5} > I^{S-Limit} \tag{3.5}$$

I^{Evans} may have reached the saturation level causing the drop in dimagnetic signal $\delta\dot{\Phi}$

4 The VDE-code for EAST to be a research tool

We have sufficient theory understanding of VDE in order to move to its numerical implementation

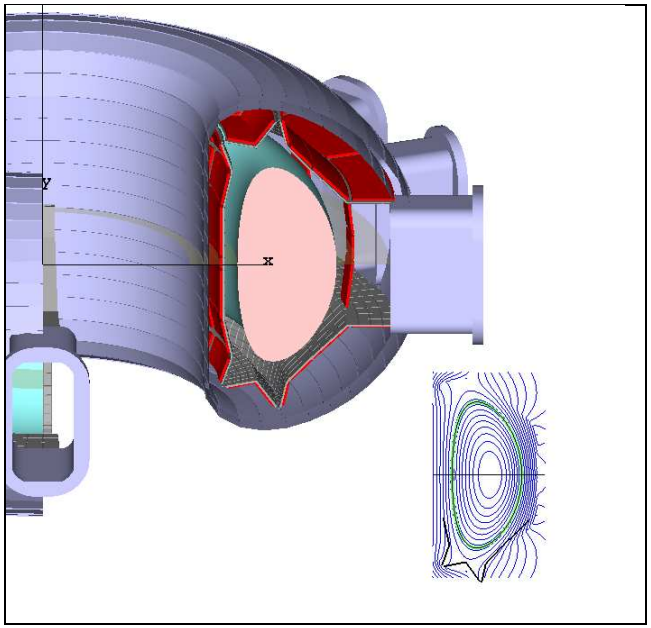

Initial unstable plasma

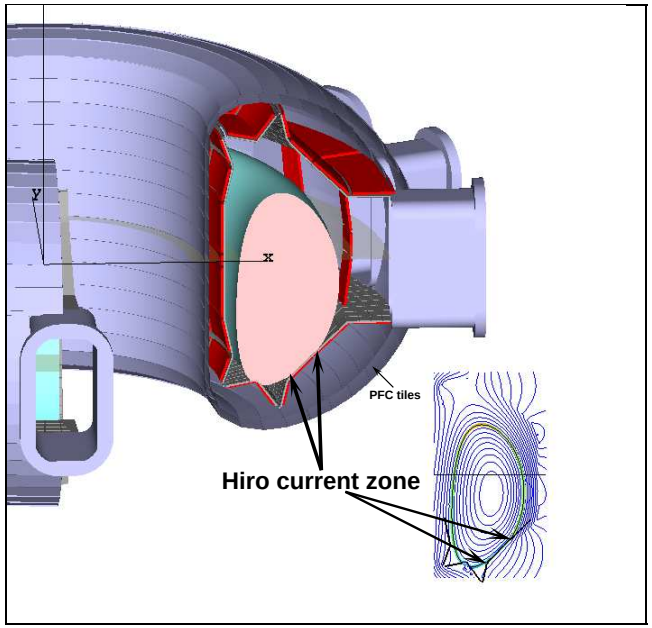

Plasma touches the divertor plate and generate Hiro currents, $\Phi/\Phi_0 = 1$

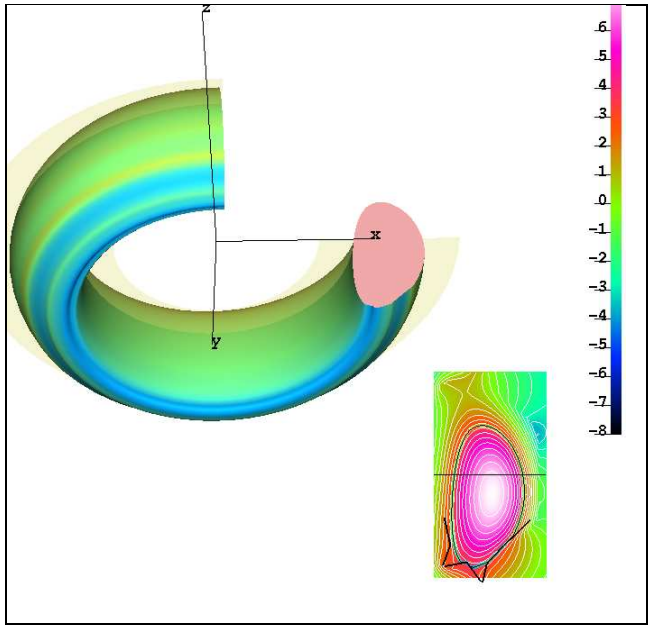

Negative Hiro currents (blue), shown in the contact area of plasma

!!! Our VDE code shows the contact zone right at the position of Xiong tiles !!!

Plasma VDE in EAST geometry

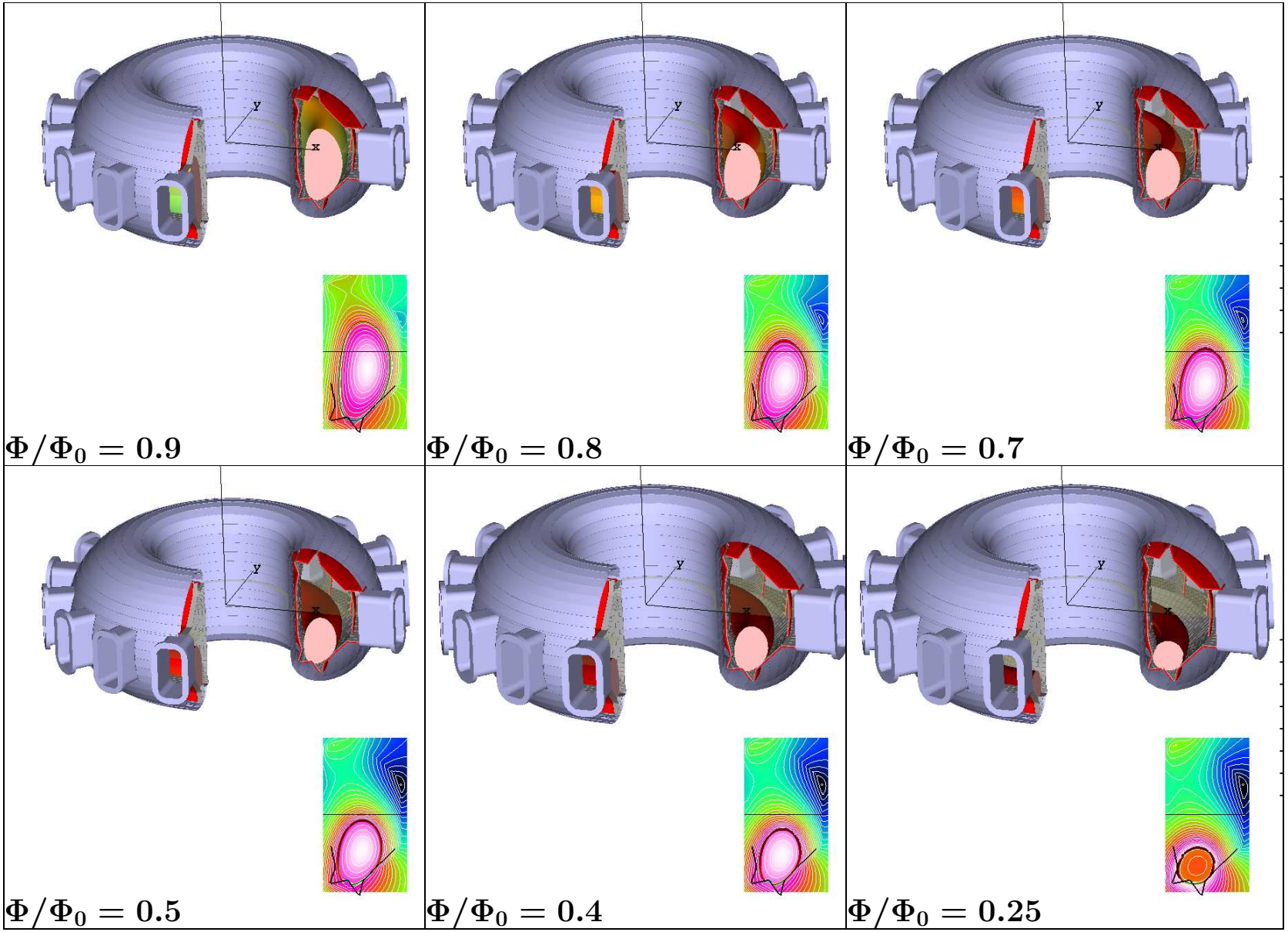

4.1 The real in-vessel geometry is an essential part

Real EAST in-vessel geometry is used for VDE simulations.

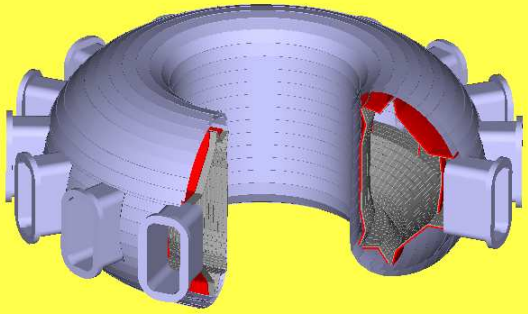

Vacuum Chamber

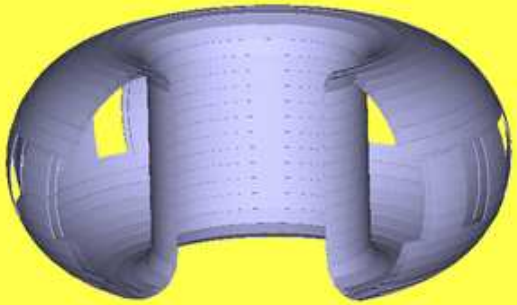

Double layer vacuum vessel

Stabilizer elements (16 toroidal sections)

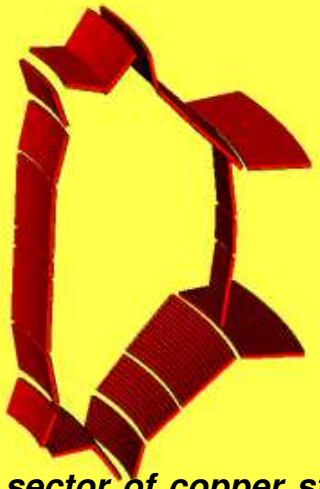

One toroidal sector of copper stabilizers (8728 triangles)

All associated Greens functions for wall circuit equations are already calculated

We have to

1. *substitute the present response of a simplistic wall by Greens functions calculations;*
2. *arrange the interfaces with EAST signals;*
3. *merge our and Lukash (DINA) experiences.*

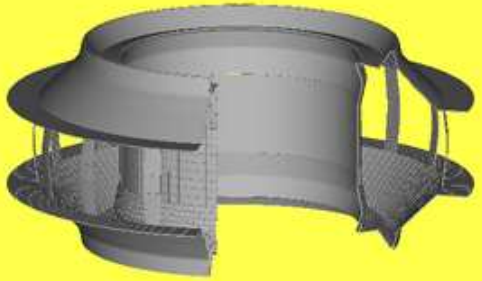

Carbon plasma facing tiles

4.2 5 regimes of the vertical instability

Classical case of vertical instability

1. *Cylindrical geometry;*
2. *Straight plasma column with a uniform current;*
3. *Elliptical cross-section*
4. *Quadrupole external field*

1. *Continuous wall (no gaps);*
2. *External equilibrium field is frozen to the wall in advance;*
3. *The wall screens magnetic perturbations from instability*

Wall Touching Vertical Mode (VDE):

1. *Tile surface is transparent to magnetic fields;*
2. *Plasma touching the tiles shortens the gaps*

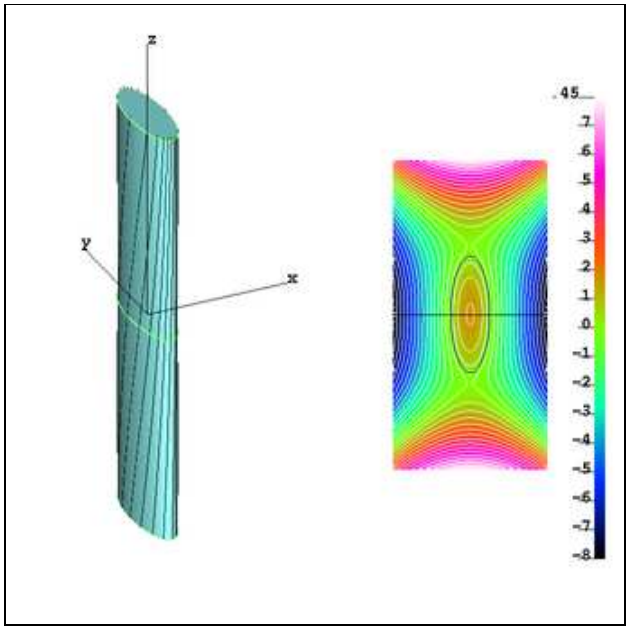

No wall, I_{pl} =const

On left: 3-D plasma geometry and On right: 2-D cross-section.
Ψ =const contours are shown in color with a plasma in the center

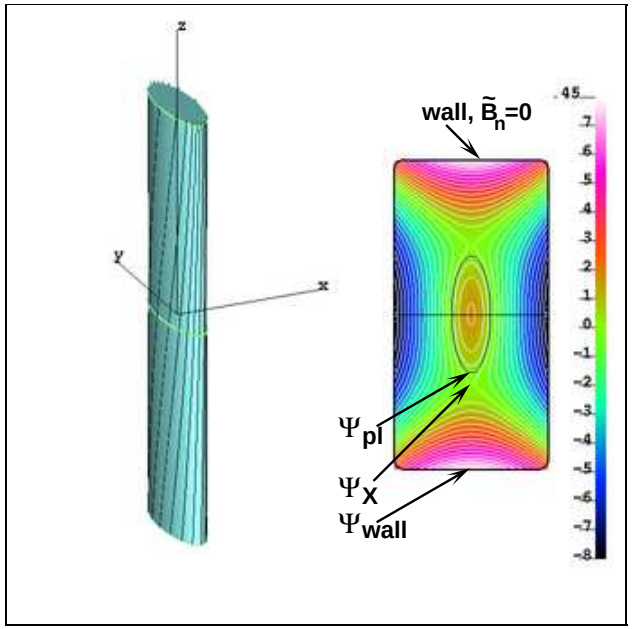

Ideally conducting wall, $\Delta\Psi\big|_{core}^{wall}$ =const

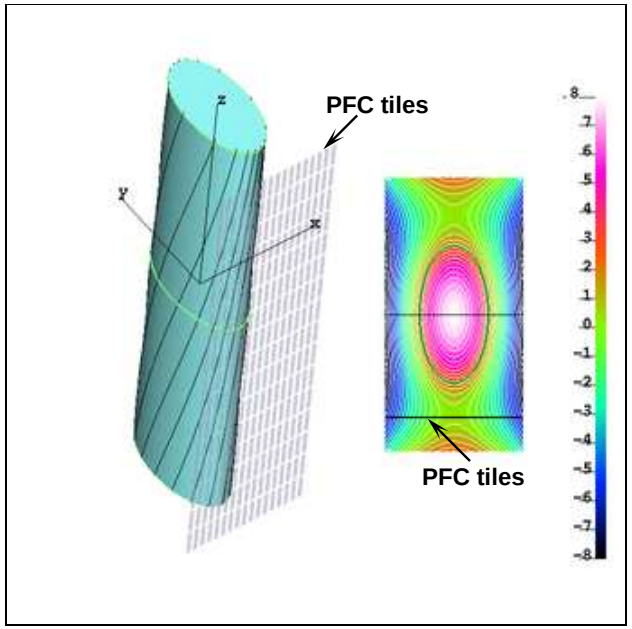

Tile surface on the path of the plasma motion.

(In absence and presence of a wall)

Case 1: No wall, No tiles

Strong external field stops the vertical motion. New geometry of reconnection is discovered

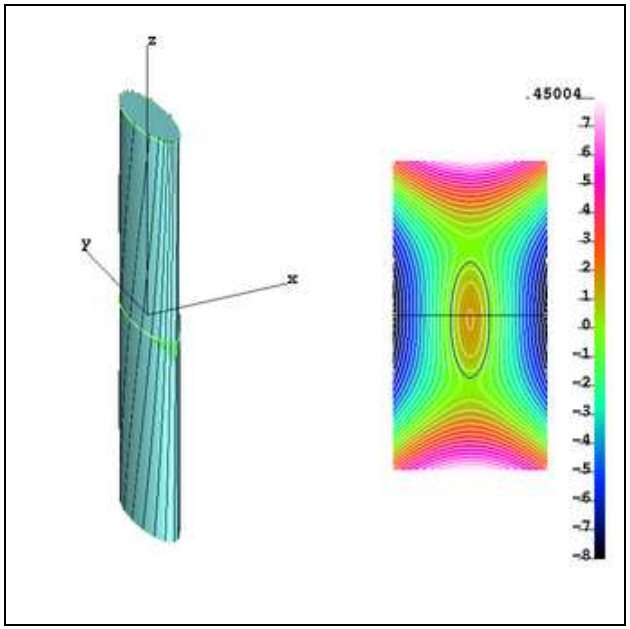

Initial downward plasma displacement

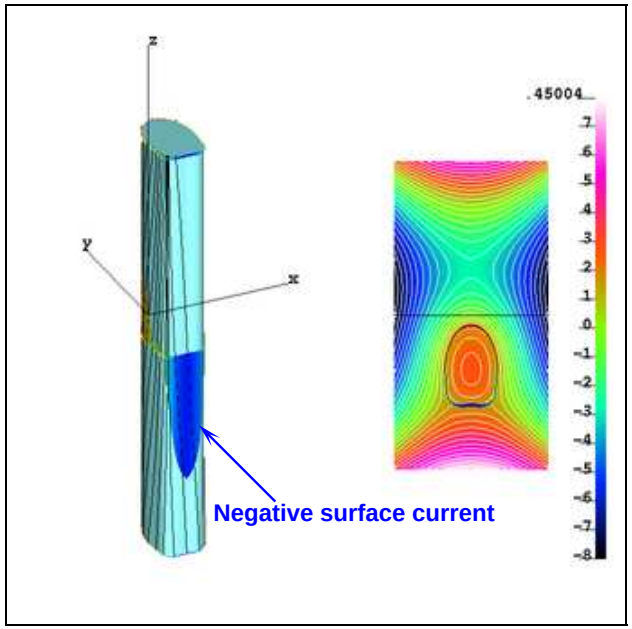

Nonlinear phase of instability. Negative surface current at the leading plasma side

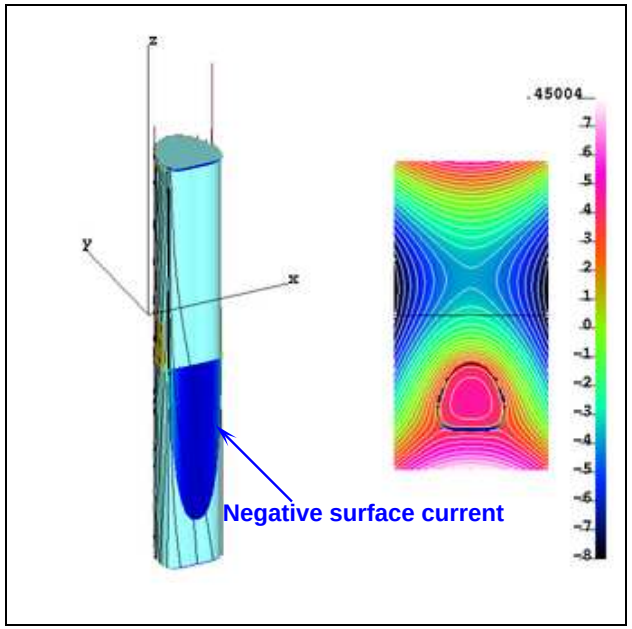

1. ***Strong negative sheet current at the leading plasma edge***
2. ***Plasma cross-section becomes triangle-like***

(a) opposite poloidal field $B_\theta^{vac} \simeq -B_\theta^{core}$ across the leading plasma edge;

(b) two Null Y-points of poloidal field in two vertices of plasma cross-section.

Plasma should be leaked through the Y-point untill full disappearance.

Case 2-a: plasma is separated from the wall

In the presence of a conducting wall, there are two different situations:

1. $|\Psi_{pl} - \Psi_X| < |\Psi_X - \Psi_{Wall}|$ ***- plasma separated from the wall***
2. $|\Psi_{pl} - \Psi_X| > |\Psi_X - \Psi_{Wall}|$ ***- plasma is close to the wall***

depending on relation between poloidal fluxes at the plasma, in X-point, and at the wall.

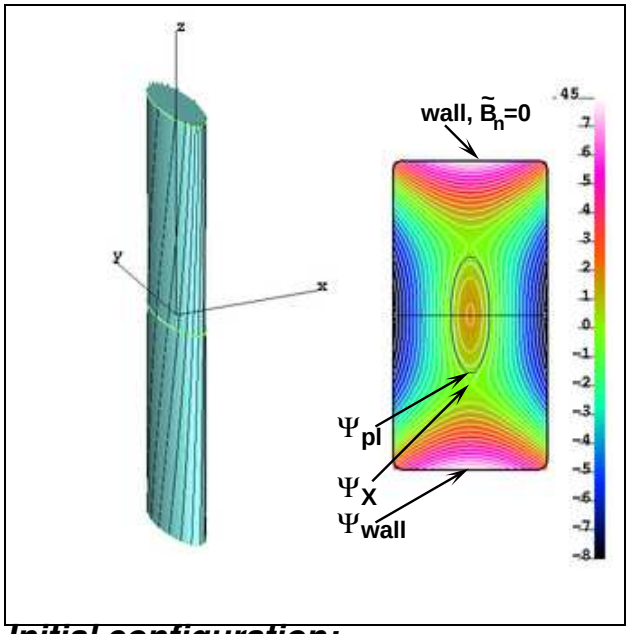

Initial configuration:
$|\Psi_{pl} - \Psi_X| < |\Psi_X - \Psi_{Wall}|$

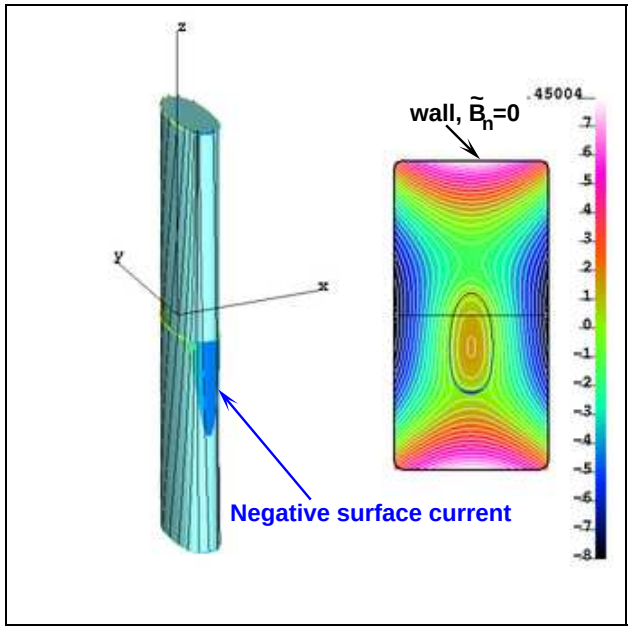

Initial downward plasma displacement

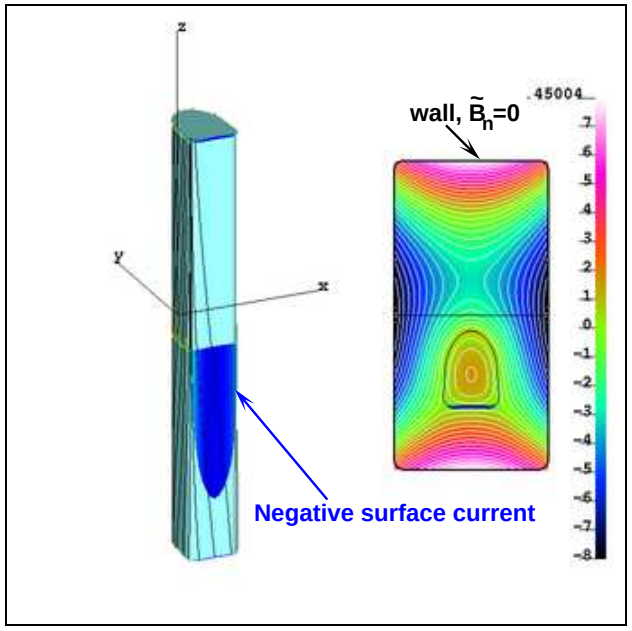

Plasma stops vertically and goes to re-connection

The motion of plasma essentially repeats the instability without wall and finally leads to a reconnection geometry

Case 2-b: plasma is close to the wall

Initially, plasma moves as in the previous case.

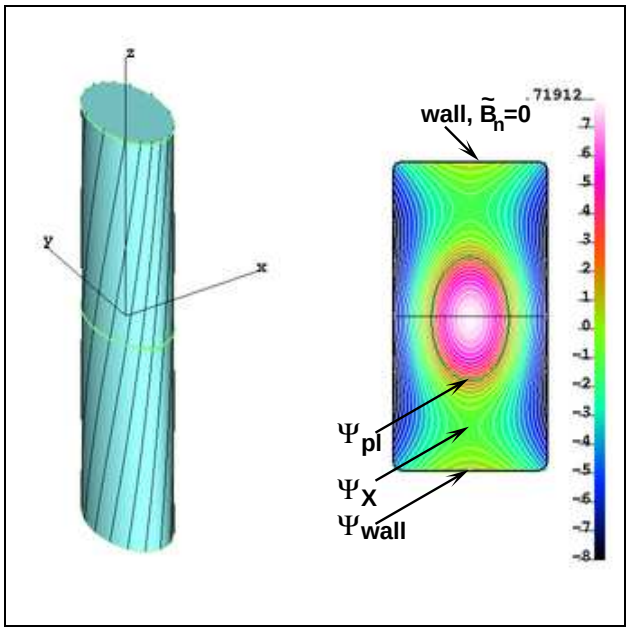

Initial configuration:
$|\Psi_{pl} - \Psi_X| > |\Psi_X - \Psi_{Wall}|$

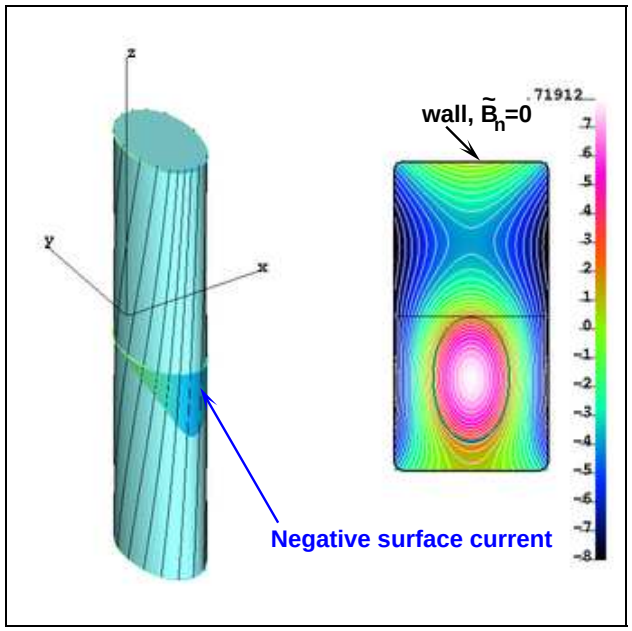

Nonlinear phase of instability. Negative surface current at the leading plasma side

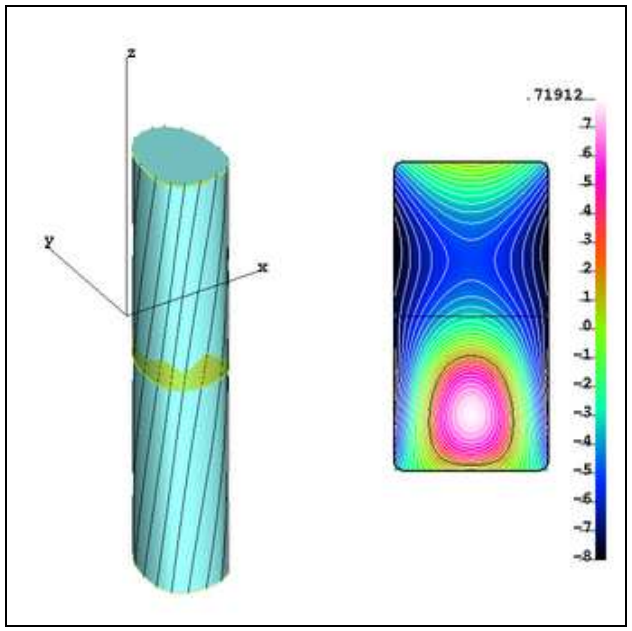

Leading side of the equilibrium plasma. Negative surface current is replaced by a positive one.

The Grad-Shafranov equilibrium codes (e.g., DINA) can simulate this "resistive-wall-mode" regime.

Case 3a: VDE with plasma facing tiles (no wall)

Surface currents at the free flowing plasma are converted to

1. ***Hiro currents affecting the instability, and***
2. ***Evans currents to the tile surface, misinterpreted as "halo" currents***

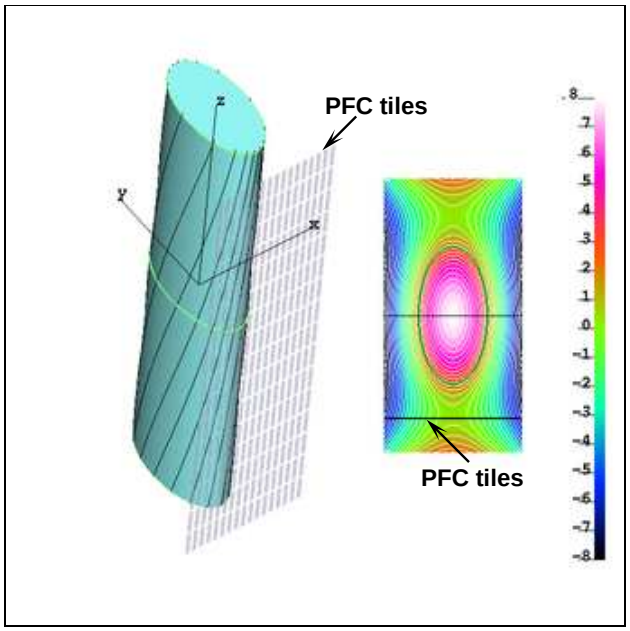

Initial downward plasma displacement

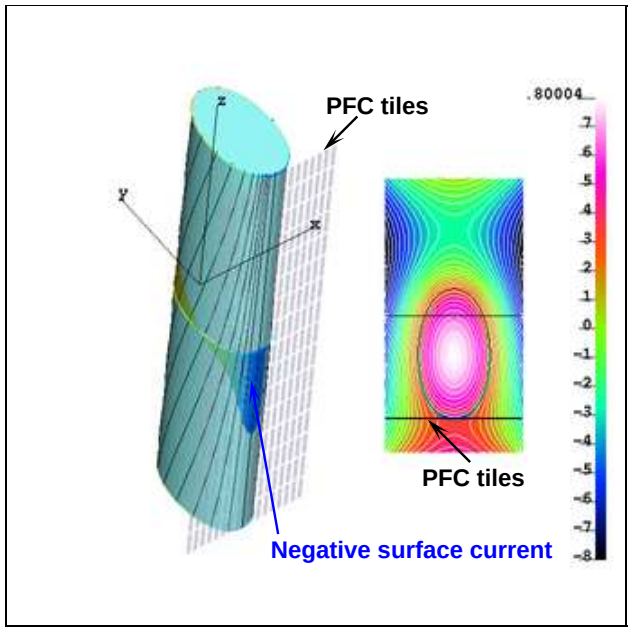

Negative surface current at the leading plasma side

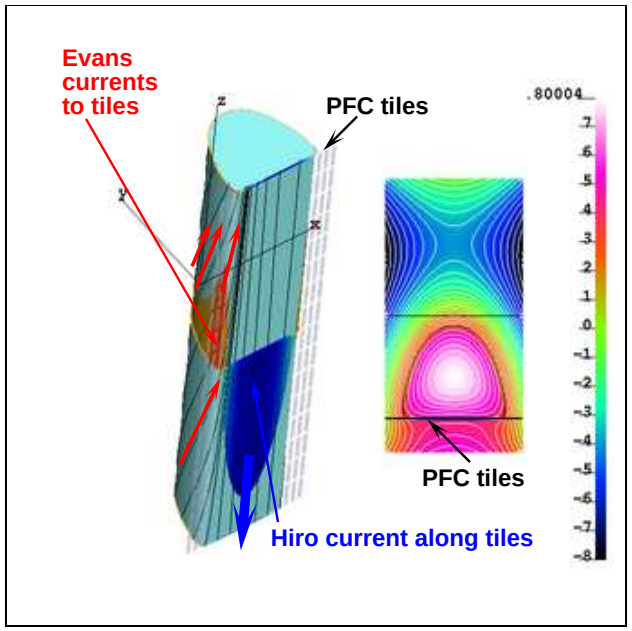

Two distant Y-points are formed at the leading edge

1. ***Negative surface currents are transformed into toroidal Hiro currents***
2. ***Positive surface currents along field lines are partially converted to Evans currents to the tile surface.***

Case 3b: VDE with tiles and a wall

In tokamaks, the plasma is always "separated" from the wall based on $\Psi_{pl}, \Psi_X, \Psi_{Wall}$.

The presence of the wall does not affect VDE significantly

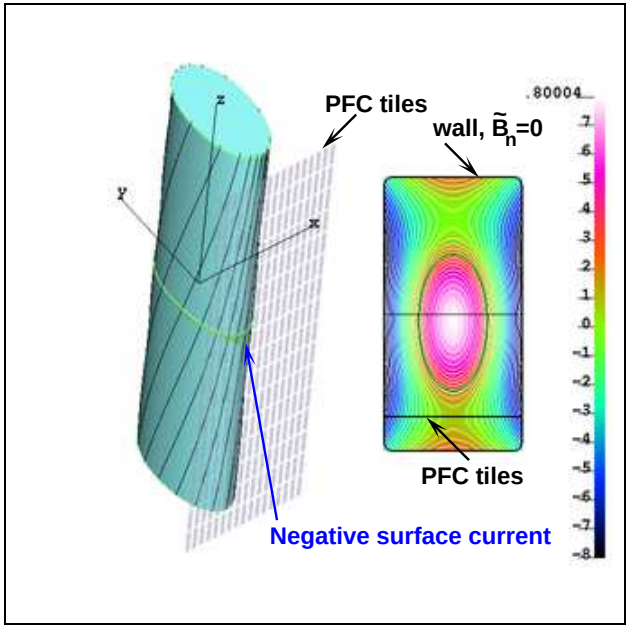

Initial plasma displacement

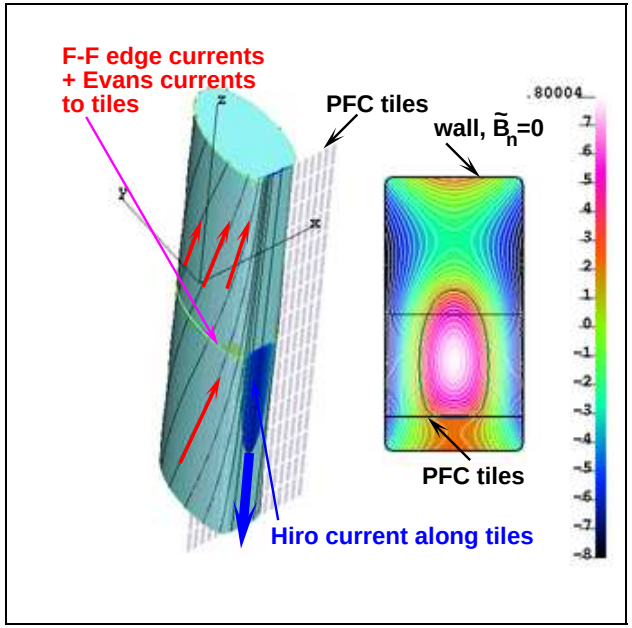

Negative surface current at the leading edge

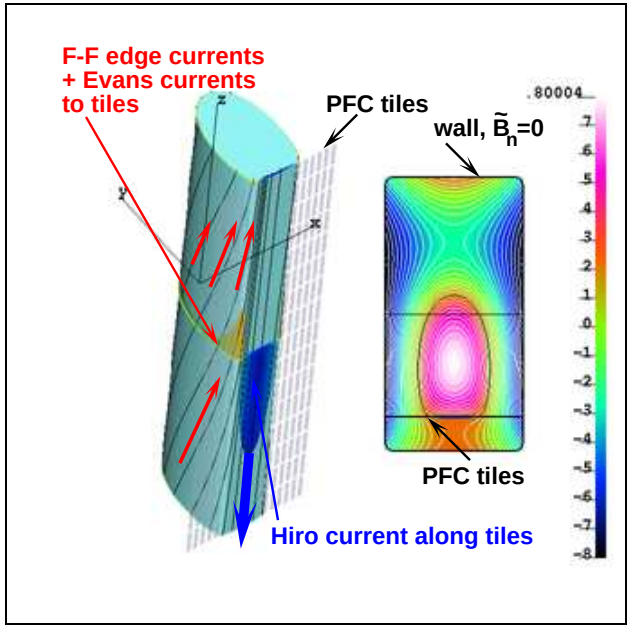

Hiro, Evans currents, formation of two Y-points

Due to stabilizing wall action, Y-points are less separated than in the absence of the wall

Otherwise, the plasma motion in both cases is similar.

5 The Tokamak MHD (TMHD)

The Tokamak MHD is presented by the following set of equations

1. ***Equation of motion is split into an equilibrium equation***

$$\nabla p = (\vec{j} \times \vec{B}), \quad \bar{\Psi} = \bar{\Psi}(\bar{\Phi}), \tag{5.1}$$

and the plasma boundary advancing equation

$$\lambda \vec{\xi} = -\frac{\bar{F}}{r^2}\nabla \tilde{F}, \quad \left(\nabla \cdot \frac{\bar{F}^2}{r^4}\nabla \tilde{F}\right) = 0. \tag{5.2}$$

2. ***Faraday's (Ohm's) law in plasma and the wall (with no $\vec{V}$)***

$$-\frac{\partial \vec{A}}{\partial t} - \nabla \varphi^E + (\vec{V} \times \vec{B}) = \frac{\vec{j}}{\sigma}, \quad \vec{V} \equiv \frac{d\vec{\xi}}{dt}. \tag{5.3}$$

3. ***Plasma anisotropy***

$$\sigma = \sigma(\bar{\Phi}), \quad (\vec{B} \cdot \nabla) \simeq 0. \tag{5.4}$$

4. ***boundary condition at the wall (determines plasma V_{normal} to the wall)***

$$\vec{E}_{\|}^{pl} = \vec{E}_{\|}^{wall} = \frac{\vec{j}^{pl}}{\sigma^{pl}} - (\vec{V} \times \vec{B}) = \frac{\vec{j}^{wall}}{\sigma^{wall}}. \tag{5.5}$$

Force balance across the free plasma surface

$$\left(p + \frac{|\vec{B}|^2}{2\mu_0} + \frac{\bar{F}\tilde{F}}{r^2\mu_0}\right)_i = \left(\frac{|\vec{B}|^2}{2\mu_0}\right)_e, \tag{5.6}$$

where subscripts 'i, e' specify the inner and outer sides of the plasma surface.

The numerical scheme of TMHD is simply beautiful

Each of all TMHD equations has its own energy principle leading to a positively defined symmetric matrix if expressed in terms of finite elements. Stability is guarantied

3-D equilibrium (3-D Hermit elements, block tri-diagonal)

$$W^{\vec{j}\times\vec{B}} \equiv \frac{1}{2}\int\left(\frac{|\vec{B}|^2}{2\mu_0} - (\vec{A}\cdot\vec{j})\right)d^3\mathrm{r}$$
$$\equiv \frac{1}{2\mu_0}\int\Big\{K(\bar{\Phi}'+\psi'_a+\bar{\Phi}'\eta'_\zeta)^2 - 2N(\bar{\Phi}'+\psi'_a+\bar{\Phi}'\eta'_\zeta)(\psi'_\theta-\phi'_\zeta)+M(\psi'_\theta-\phi'_\zeta)^2 \qquad (5.7)$$
$$+Q(\bar{\Phi}'+\phi'_a+\bar{\Phi}'\eta'_\theta)^2 - 2\tilde{N}(\bar{\Psi}'+\psi'_a+\bar{\Phi}'\eta'_\zeta)(\bar{\Phi}'+\phi'_a+\bar{\Phi}'\eta'_\theta)$$
$$+2\tilde{M}(\psi'_\theta-\phi'_\zeta)(\bar{\Phi}'+\phi'_a+\bar{\Phi}'\eta'_\theta) - (\bar{\Phi}+\phi)\hat{F}'_a + (\bar{\Psi}+\psi)(\hat{J}'_a+\nu'_\theta)\Big\}\,da d\theta d\zeta.$$

Plasma advancing (3-D Hermit elements, block tri-diagonal)

$$W^F = \frac{1}{2}\int \bar{F}^2\frac{g^{aa}\tilde{F}'^2_a + 2g^{a\theta}\tilde{F}'_a\tilde{F}'_\theta + g^{\theta\theta}\tilde{F}'^2_\theta + 2g^{a\zeta}\tilde{F}'_a\tilde{F}'_\zeta + 2g^{\theta\zeta}\tilde{F}'_\theta\tilde{F}'_\zeta + g^{\zeta\zeta}\tilde{F}'^2_\zeta}{r^4}J da d\theta d\zeta. \qquad (5.8)$$

Faraday's law (3-D Hermit elements, block tri-diagonal)

$$W^t = \frac{1}{2}\int\left\{\frac{\partial}{\partial t}\left(KB^\theta B^\theta + 2\tilde{M}B^\theta B^\zeta + QB^\zeta B^\zeta\right) + \eta^{pl}\left(Kj^\theta j^\theta + 2\tilde{M}j^\theta j^\zeta + Qj^\zeta j^\zeta\right)\right\}d^3r. \qquad (5.9)$$

Sink/source wall current from the plasma (triangle based wall model, small sparse matrix)

$$W^S = \int\left\{\frac{\bar{\sigma}(\nabla\phi^S)^2}{2} + j_\perp\phi^S\right\}dS - \frac{1}{2}\oint\phi^S\bar{\sigma}[(\vec{n}\times\nabla\phi^S)\cdot d\vec{l}]. \qquad (5.10)$$

Hiro, eddy currents in the wall (triangle based wall model, stationary matrix)

$$W^I \equiv \frac{1}{2}\int\left\{\frac{\partial(\vec{\imath}\cdot\vec{A}^I)}{\partial t} + \bar{\eta}|\nabla I|^2 + 2\left(\vec{\imath}\cdot\frac{\partial\vec{A}^{ext}}{\partial t}\right)\right\}dS - \oint(\phi^E-\phi^S)\frac{\partial I}{\partial l}dl. \qquad (5.11)$$

Force balance versus plasma inertia in disruptions

In contrast to TMHD, the numerical in existing 3-D MHD codes are driven by the equation of motion

$$\rho\frac{d\vec{V}}{dt} = -\nabla p + (\vec{j}\times\vec{B}) + \textit{(hyper-) viscosity} \qquad (5.12)$$

with a huge 4 decade old problem of Courant time step limitations.

JET discharge parameters of 38070:

n_e	$\simeq 3\cdot 10^{19}$	*plasma density*
V_{olume}	$\simeq 60$ *m*^{3}	*plasma volume*
ξ	< 0.3 *m*	*amplitude of the m/n=1/1 perturbation*
Δt	*25 ms*	*duration of m/n=1/1 perturbation*
F_x	$\simeq 2.4$ *MN*	*the sideways force*

Force of plasma inertia

$$F_\rho \simeq m_i n_i \cdot V_{olume}\cdot\frac{2\xi}{(\Delta t)^2} \simeq 0.006\ [N] \quad \ll 2.4\cdot 10^6 [N]. \qquad (5.13)$$

The mismatch between 3-D code models and the tokamak reality is 10^8 in driving forces or 10^4 in the time scale

There is no a possible use of existing 3-D MHD codes, hydrodynamic in nature.

The trick M3D uses is a hidden enhancement of ITER 15 MA current to the level of 24 MA, not reflected in the title, abstract, introduction, summary and in presentations

Now the practical approach for TMHD codes, consistent with the tokamak physics, was formulated (PPPL, FAR-TECH, ICM&SEC)

Free-boundary equilibria with ESC-EEC

ESC-EEC can calculate free-boundary equilibria in both $r - z$ and flux coordinates

The Equilibrium Spline Interface (ESI) is developed for equilibrium codes instead of present mess in interfacing

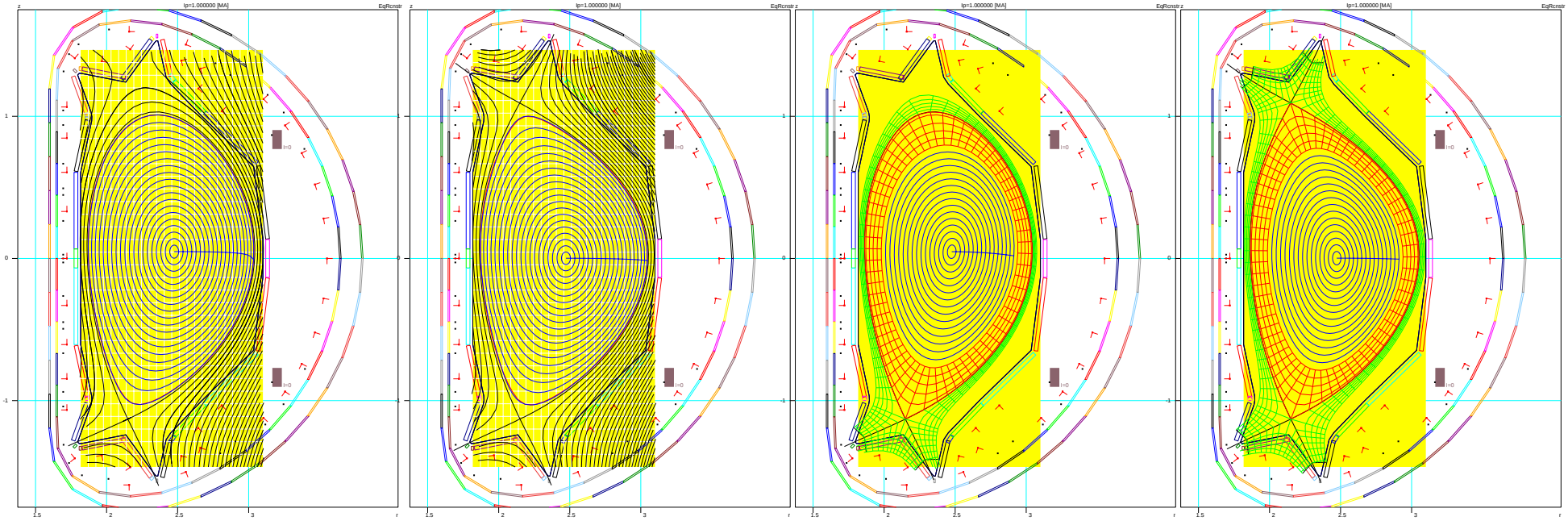

(a) ID=00,1,00,00,00 ***(b) ID=00,01,00,00,00*** ***(c) ID=00,40,00,00,23*** ***(d) ID=00,40,00,00,23***

Free boundary ESC-EEC is a step for inclusion of going beyond δ-functional TMHD toward development of the physics of the Evans currents in the halo-zone

5.1 TMHD and VDE-code motivate new diagnostics

We suggested a comprehensive set of innovative tile diagnostics for Hiro, Evans and SoL current measurements on NSTX-U

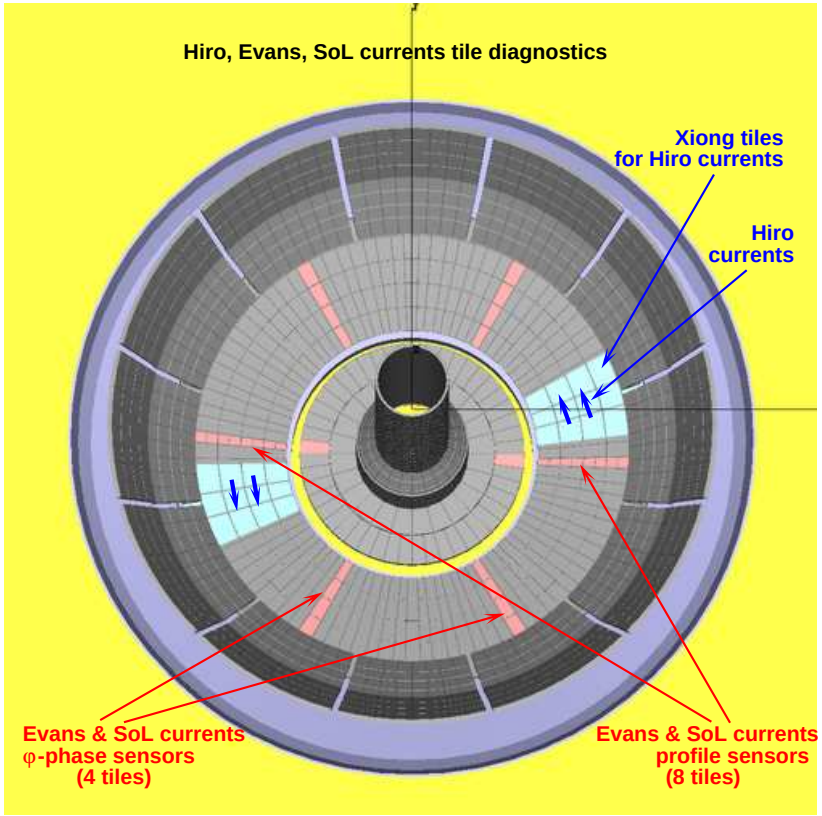

Tile sensors for measuring Hiro, Evans, and SoL currents and different kinds of diagnostics including

1. ***Hiro current diagnostics***
2. ***Evans current profile diagnostics with enhanced radial resolution***
3. ***Evans current φ-phase diagnostics***
4. ***SoL current measurements***

Evans currents carry important information on plasma-PFC interactions, never touched

6 Summary

1. ***TMHD created a credible, predictive understanding of VDEs in tokamaks, consistent with observatons and extendable to more details in physics***
2. ***New set of MHD equations, compact and rational, is derived for VDE***
3. ***New stable and fast numerical are formulated for implementation***
4. ***2-D version of the VDE code is operational and on the way to be a research tool for the EAST tokamak.***
5. ***New tile diagnostics are motivated for tokamak disruptions***

This prepare a transition to further progress in disruption understanding, which will require the close cooperation of theory, numerical simulations and experimental measurements and interpretations

Hiro currents in Large disruption shot 38070

Regarding the use of "halo" currents for currents, specific to VDEs:

- *Based on the plasma physics, it is not possible to confuse the Hiro currents with the "halo" currents:*

$$\int (I_7 - I_3)_{38070} dt = \int I_{38070}^{Hiro} dt = 4350\ [A \cdot s] \gg 600 \qquad (6.1)$$

In the shadow plasma the electric charge is probably another two orders of magnitude smaller.

In contrast to "halo-", the Hiro-currents are NOT limited the electric charge

- *The Evans currents are a specific kind of halo-currents*
- *Neither Evans- nor what would be other halo- currents exert appreciable VDE forces.*

Although it is impossible to affect the misuse of "halo current" term in this community, the "halo"-name as a substitution of "Hiro" is highly confusing and works against the progress.

The major concern at the moment is that the potentially big effect of the Hiro currents on the Be plasma facing tiles in ITER is being overlooked in its disruption analysis